Brillouin-scattering cross sections of off-axis phonons in CdS

Ole Keller
Physics Laboratory, Royal Veterinary and Agricultural University, Copenhagen, Denmark
(Received 18 July 1974)

Incorporating the rotational contribution to the direct photoelastic effect and the angular deviation of the Poynting vector from the wave vector of the diffracted light a Brillouin-scattering theory, valid for a general anisotropic scattering kinematics in a hexagonal crystal, is derived. From the basic theory Brillouin-scattering cross sections of off-axis pure transverse (T_1), quasitransverse (T_2), and quasilongitudinal (L) phonons are calculated in the cases where the optic axis lies in the scattering plane and the incident light is polarized either parallel or perpendicular to this plane. The frequency dependence and the angular dependence of the cross section for visible light ($\lambda_0 = 6328$ Å) in CdS are evaluated for a number of important cases. The main emphasis of the numerical calculations is devoted to the T_1 mode for which the scattering cross section has one, two, or four branches. For certain scattering geometries the cross section equals zero for selected phonon frequencies and off-axis angles. It is shown that an experimental determination of the relative signs of the symmetric photoelastic tensor components conveniently can be based on a localization of the zeros for the L-phonon scattering cross section. The formulas derived in the present paper are very useful for an analysis of the frequency spectrum and the angular distribution of the phonons in acoustoelectrically active or inactive off-axis domains in hexagonal crystals like CdS and ZnO.

I. INTRODUCTION

The diffraction of light by elastic waves in solids was predicted by Brillouin[1] in 1922 and observed some eight years later.[2,3] In the following period the effect was extensively studied both experimentally and theoretically. A renewed interest in the subject was triggered off by the advent of the laser as a source for producing coherent optical radiation and the techniques for generating acoustic waves in the microwave region.[4–6] Originally, Brillouin scattering was mainly used to determine elastic constants and ultrasonic attenuation.[6–9] Later on, a comparative Brillouin-scattering technique was used to evaluate symmetric[10,11] and antisymmetric[12] photoelastic tensor components. In 1966, Zucker and Zemon[13] applied Brillouin scattering in a study of nonthermal phonon distributions generated in some piezoelectric semiconductors via the acoustoelectric coupling. Today, Brillouin scattering has turned out to be the most powerful method for investigating a number of acoustic properties of acoustoelectric domains. The aspects which can be studied with advantage by light scattering include: (i) the time development of the different frequency and angular plane-wave components of on-axis and off-axis domains in the weak- and strong-flux regions,[13–20] (ii) parametric interactions,[17,18,21,22] (iii) two-dimensional properties of domains,[20,23,24] (iv) anisotropy effects,[23–26] (v) phonon focusing,[23,24,26] (vi) properties of acoustoelectrically inactive domains,[27] (vii) nonelectronic attenuation of T_1, T_2, and L phonons,[17,27,28] (viii) regeneration effects,[23,29] (ix) domain velocity,[30] and (x) multipeak domain propagation.[30,31]

The use of Brillouin scattering as an optical probe in these studies requires a detailed knowledge of the scattering kinematics[20,32] and the scattering cross section.[20,33]

In optically isotropic solids the kinematics is determined by the normal Bragg condition,[1–3] whereas the scattering geometry in anisotropic media is calculated on the basis of the anisotropic Bragg laws derived by Dixon.[34] Deviations from the normal Bragg law occur if (i) there is a polarization rotation of light in the scattering process,[34] if (ii) the refractive index depends on the propagation direction of light,[35] or if (iii) the scattering event involves a combination of (ii) and (iii).[32]

In this work we evaluate and discuss the Brillouin-scattering cross section of off-axis and on-axis T_1, T_2, and L phonons in hexagonal crystals. The scattering plane contains the c axis and the incident light is polarized either parallel or perpendicular to this plane. The frequency dependence of the scattering cross sections will be discussed on the basis of numerical results for CdS. Boundary effects will not be considered. The present model is based on the theory of Brillouin-scattering cross sections given by Hamaguchi,[33] and the theory of anisotropic Brillouin-scattering kinematics developed by Keller and Søndergaard.[32]

Based on Green's-function techniques a general theory of Brillouin scattering in anisotropic media which includes boundary effects has been published by Nelson *et al.*[12] Using an integral-equation method, Hope[36] incorporates birefringence, depletion of the incident beam, and multiple internal reflections in his theory. Unfortunately, the above theories are too complicated to be applied to elastic waves

with arbitrary polarization and propagation directions. A Brillouin-scattering theory for cubic crystals has been given by Benedek and Fritsch.[37]

II. BRILLOUIN-SCATTERING CROSS SECTIONS IN HEXAGONAL CRYSTALS

If a beam of light passes through a solid, a fraction of the incident light will be scattered in specific directions determined by the spatial Fourier components of the thermal[37] or nonthermal[38] time-space fluctuations in the dielectric constant of the medium. In strong piezoelectric semiconductors three effects can contribute significantly to the fluctuations of the dielectric constant, i.e.,

$$\delta\overleftrightarrow{\epsilon}^{\,\mathrm{tot}} = \delta\overleftrightarrow{\epsilon}^{\,D}_{\mathrm{ph}} + \delta\overleftrightarrow{\epsilon}^{\,I}_{\mathrm{ph}} + \delta\overleftrightarrow{\epsilon}_{\mathrm{el}}. \tag{1}$$

The first term, $\delta\overleftrightarrow{\epsilon}^{\,D}_{\mathrm{ph}}$, arising from the fluctuations in the strain tensor[39] and the mean rotation tensor[40] gives the direct photoelastic effect. The second term, $\delta\overleftrightarrow{\epsilon}^{\,I}_{\mathrm{ph}}$, represents the indirect photoelastic effect, that is, the succession of the piezoelectric and electro-optic effects.[12,41] Since $\delta\overleftrightarrow{\epsilon}^{\,I}_{\mathrm{ph}}$ is a tensor function of the acoustic wave-vector direction, the indirect photoelastic effect has different symmetry than the direct effect. Although the indirect photoelastic effect can be comparable in magnitude with the direct effect in strong piezoelectric semiconductors as CdS and ZnO,[42] it has been forgotten in all previous Brillouin-scattering analyses.[19,20,24,33] The third term, $\delta\overleftrightarrow{\epsilon}_{\mathrm{el}}$, gives the free-electron contribution to the fluctuations in the dielectric constant. The electronic term can be comparable in magnitude to $\delta\overleftrightarrow{\epsilon}^{\,D}_{\mathrm{ph}}$ for the bunched electrons in a fully developed acoustoelectric domain in CdS if the 10.6-μm line of a CO_2 laser is used as the radiation source.[43] All the acoustic modes (T_1, T_2, L) can contribute to $\delta\overleftrightarrow{\epsilon}^{\,D}_{\mathrm{ph}}$,[20,33,39,40] whereas only the piezoelectrically active T_2 and L modes can contribute to $\delta\overleftrightarrow{\epsilon}^{\,I}_{\mathrm{ph}}$ and $\delta\overleftrightarrow{\epsilon}_{\mathrm{el}}$.[12,41-43] Light scattered from the lattice can be subjected to a polarization rotation[20,32,33,36] and is, in general, out of phase with the unrotated light scattered from the solid-state plasma.[43,44]

In the present work, we discuss Brillouin scattering via the direct photoelastic effect only. For visible light or infrared radiation a solid can be regarded as a continuum, justifying a classical calculation of the scattered light intensity. Using the integral-equation method, Benedek and Fritsch have analyzed the Brillouin scattering from cubic crystals.[37] Incorporating birefringence this theory has been extended to hexagonal crystals and applied to acoustic waves propagating parallel or perpendicular to the c axis by Hamaguchi.[33] The present theory modifies the work of Hamaguchi to include the rotational effect,[40] and the general theory is applied to off-axis acoustic waves. The derivation of the Brillouin-scattering cross section is based on the assumption that the attenuation of the incident light is negligible. This approximation is not justified if we are dealing with intense scattering effects.[17]

An incident electric field

$$\vec{E}_i(\vec{r}, t) = \vec{E}_0 e^{i(\vec{k}_i\cdot\vec{r}-\omega_i t)} \tag{2}$$

produces an oscillating polarization, which in turn radiates electromagnetic energy. By (i) assuming a low-intensity incident radiation so that the local polarization is linearly proportional to the electric field, by (ii) realizing that the characteristic frequencies for the lattice fluctuations are small ($\lesssim 10^{12}$ Hz) compared to the light frequency in the optical region ($\sim 10^{14}$–10^{15} Hz), and by (iii) accounting for the time retardation, the far-field diffracted electric field, from a scattering volume $V_s = 1$, at a point $\vec{R}$ is given by

$$\vec{E}_d(\vec{R}, t) = -\left(\frac{\omega_i}{c}\right)^2 \frac{(2\pi)^{3/2}}{4\pi R} \times \sum_{\mu} \left(e^{i[\vec{k}_d\cdot\vec{R}-(\omega_i \pm \Omega^{\mu}(\vec{q}))t]}\, \hat{k}_d \times\{\hat{k}_d\times[\delta\overleftrightarrow{\epsilon}^{\,\mu}(\vec{q})\circ\vec{E}_0]\}\right), \tag{3}$$

where ω_i and c are the angular frequency and the velocity of light in vacuum. The wave vectors of the incident photon ($\vec{k}_i$) and the diffracted photon ($\vec{k}_d$) are given by

$$\vec{k}_i = (n_i/c)\omega_i \hat{k}_i \tag{4}$$

and

$$\vec{k}_d = (n_d/c)[\omega_i \pm \Omega^{\mu}(\vec{q})]\,\hat{k}_d, \tag{5}$$

where n_i and n_d are the refractive indices of the incident and scattered light, and $\hat{k}_i$ and $\hat{k}_d$ are unit vectors in the direction of the incident and scattered wave. The wave vector and angular frequency of the scattering fluctuation (phonon) which in particular is responsible for the scattering of light into the direction $\hat{k}_d$ are $\vec{q}$ and $\Omega^{\mu}(\vec{q})$. The index μ labels the different branches in the phonon dispersion relation connecting $\vec{q}$ and $\Omega^{\mu}(\vec{q})$. In general, $\Omega^{\mu}(\vec{q})$ can be complex to include a description of the damping of the fluctuations. The plus sign corresponds to a phonon-absorption process, the minus sign to a phonon-emission process. Expressing the fluctuations in the dielectric constant, $\delta\overleftrightarrow{\epsilon} \equiv \delta\overleftrightarrow{\epsilon}^{\,D}_{\mathrm{ph}}$, in terms of their spatial Fourier components,

$$\delta\overleftrightarrow{\epsilon}(\vec{r}, t) = \frac{1}{(2\pi)^{3/2}} \sum_{\mu} \int \delta\overleftrightarrow{\epsilon}^{\,\mu}(\vec{q})\, e^{i[\vec{q}\cdot\vec{r}\mp\Omega^{\mu}(\vec{q})t]}\, |d\vec{q}|, \tag{6}$$

the wave vector ($\vec{q}$) of the Fourier component $\delta\overleftrightarrow{\epsilon}^{\,\mu}(\vec{q})$ which produces the scattering in the direction $\hat{k}_d$ satisfies the implicit equation

$$\vec{k}_d = \vec{k}_i \pm \vec{q}. \tag{7}$$

Equations (5) and (7) represent the conservation of

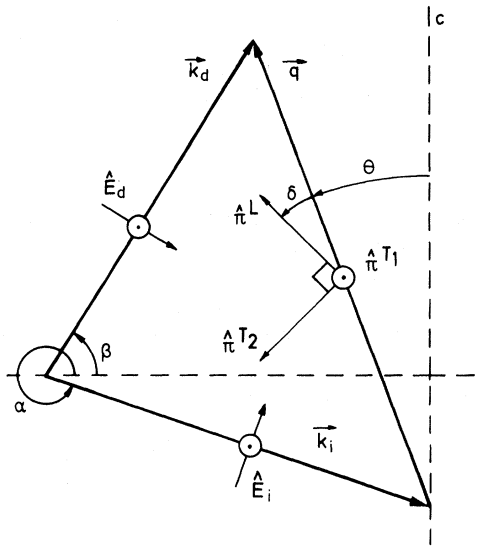

FIG. 1. Pseudomomentum conservation diagram for a T_1-, T_2-, or L-phonon absorption process in a scattering configuration containing the c axis. The unit vectors $\hat{E}_i$ and $\hat{E}_d$ in the polarization directions of the incident photon ($\vec{k}_i$) and the diffracted photon ($\vec{k}_d$) are either parallel or perpendicular to the scattering plane. The off-axis T_1, T_2, or L phonons are characterized by the unit vectors $\hat{\pi}^{T_1}$, $\hat{\pi}^{T_2}$, and $\hat{\pi}^L$ in the directions of the particle displacement. The deviation of the T_2 and L modes from pure modes is given by $\delta = \delta(\theta)$.

energy and pseudomomentum between the incident photon, the scattered photon, and the acoustic phonon. From the conservation laws one can obtain the anisotropic Bragg equations for an acoustic mode μ of frequency f[32]:

$$\sin(\theta - \alpha) = \frac{\lambda_0}{2n_i(\alpha)V_p^\mu(\theta)}\left(f + \frac{[V_p^\mu(\theta)]^2}{\lambda_0^2 f}[n_i^2(\alpha) - n_d^2(\beta)]\right) \tag{8}$$

and

$$\sin(\beta - \theta) = \frac{\lambda_0}{2n_d(\beta)V_p^\mu(\theta)}\left(f - \frac{[V_p^\mu(\theta)]^2}{\lambda_0^2 f}[n_i^2(\alpha) - n_d^2(\beta)]\right), \tag{9}$$

where the angles α, β, and θ are used to determine the propagation directions of the incident photon, the scattered photon, and the phonon in the scattering plane (see Fig. 1). The direction-dependent acoustic phase velocity is $V_p^\mu(\theta)$, and λ_0 is the vacuum wavelength of the incident light. If the refractive index of light is direction independent, Eqs. (8) and (9) are reduced to the isotropic Bragg law. Based on the anisotropic Bragg equations an analysis of the Brillouin-scattering kinematics for T_1, T_2, and L phonons in some important scattering configurations has been carried out elsewhere.[32]

The intensity and the spectral distribution of the scattered radiation are determined by the autocorrelation function for the scattered electric field. Emphasizing the dependence of the scattered field on the direction of scattering, i.e., relabeling $\vec{E}_d(\vec{R}, t) = \vec{E}_d(\vec{q}, t)$, the total power in all frequencies scattered into a solid angle $d\Omega$ at the field point $\vec{R}$ is

$$dI_{sc}(\vec{q}, \vec{R}) = \frac{c_d}{8\pi}\left\langle \sum_{i=1}^{3} \epsilon_{ii} \left| E_{d,i}(\vec{q}, t) \right|^2 \right\rangle R^2 \, d\Omega, \tag{10}$$

where c_d is the direction-dependent phase velocity of the diffracted beam, and ϵ_{ii} is the appropriate component of the dielectric-constant tensor in the absence of strains. In general, for small strains, we can express the change in the dielectric-tensor components $\delta\epsilon_{ij}(\vec{r}, t)$ arising from the direct photoelastic effect as a linear function of the symmetric and antisymmetric combination of displacement gradients, i.e.,[40]

$$\delta\epsilon_{ij}^\mu(\vec{r}, t) = -\epsilon_{ii}\epsilon_{jj}\left(\sum_{l,m=1}^{3} (p_{(ij)(lm)}S_{(lm)}^\mu + p_{(ij)[lm]}R_{[lm]}^\mu)\right), \tag{11}$$

where the first term gives Pöckels contribution[39] to the direct photoelastic effect and the second term gives the rotational contribution.[40] The infinitesimal strain and mean rotation are defined, respectively, by $S_{(lm)}^\mu = \frac{1}{2}(u_{lm}^\mu + u_{ml}^\mu)$ and $R_{[lm]}^\mu = \frac{1}{2}(u_{lm}^\mu - u_{ml}^\mu)$. Parentheses enclosing subscripts indicate symmetry upon interchange of the subscripts, while brackets indicate antisymmetry upon interchange. From Eq. (11) it follows that the natural measure of elastic deformation relevant to the direct photoelastic effect is the displacement gradient $u_{kl}^\mu \equiv \partial u_k^\mu / \partial r_l$, $\vec{u}^\mu$ and $\vec{r}$ being the displacement and position vectors of a volume element of the crystal. For hexagonal crystals the generalized photoelastic tensor, defined by $(\delta\overleftrightarrow{\epsilon}^{-1})_{ij} = p'_{ijkl}u_{kl}^\mu$, equals $p_{(ij)(kl)}$ except that in place of p_{44} (contracted matrix notation) there are now two tensor elements, p'_{44} and $p'_{\bar{4}\bar{4}}$.[40] The components of the photoelastic tensor $p_{(ij)(kl)}$ for crystals with hexagonal symmetry are given by

$$\overleftrightarrow{p} = \begin{vmatrix} p_{11} & p_{12} & p_{13} & 0 & 0 & 0 \\ p_{12} & p_{11} & p_{13} & 0 & 0 & 0 \\ p_{31} & p_{31} & p_{33} & 0 & 0 & 0 \\ 0 & 0 & 0 & p_{44} & 0 & 0 \\ 0 & 0 & 0 & 0 & p_{44} & 0 \\ 0 & 0 & 0 & 0 & 0 & \frac{1}{2}(p_{11} - p_{12}) \end{vmatrix}. \tag{12}$$

The dielectric-constant tensor in the absence of phonons is

$$\overleftrightarrow{\epsilon} = \begin{vmatrix} \epsilon_{11} & 0 & 0 \\ 0 & \epsilon_{11} & 0 \\ 0 & 0 & \epsilon_{33} \end{vmatrix}, \tag{13}$$

with $\epsilon_{11} = n_o^2$ and $\epsilon_{33} = n_e^2$, n_o and n_e being the ordinary

and extraordinary refractive indices. An explicit expression for the antisymmetric part of the total photoelastic tensor is given by[40]

$$p_{(ij)[kl]} = \tfrac{1}{2}[(\epsilon^{-1})_{il}\delta_{kj} + (\epsilon^{-1})_{lj}\delta_{ik} - (\epsilon^{-1})_{ik}\delta_{lj} - (\epsilon^{-1})_{kj}\delta_{il}]. \tag{14}$$

Inserting Eq. (13) in Eq. (14) we obtain for hexagonal crystals

$$p'_{44} = p_{44} + \tfrac{1}{2}(n_e^{-2} - n_o^{-2}) \tag{15}$$

and

$$p'_{4\bar{4}} = p_{44} - \tfrac{1}{2}(n_e^{-2} - n_o^{-2}). \tag{16}$$

Using Eqs. (12)–(14), Eq. (11) can be written

$$\begin{aligned} -\delta\epsilon_{ij}(\vec{r}, t) = \sum_{m=1}^{3} p_{im}\epsilon_{ii}^2 u_{mm}^{\mu}\delta_{ij} + \epsilon_{11}^2 \tfrac{1}{2}(p_{11} - p_{12}) \\ \times(\delta_{i1}\delta_{j2} + \delta_{i2}\delta_{j1})(u_{ij}^{\mu} + u_{ji}^{\mu}) + \epsilon_{11}\epsilon_{33}\delta_{j3} \\ \times(\delta_{i1} + \delta_{i2})(p'_{44}u_{ij}^{\mu} + p'_{4\bar{4}}u_{ji}^{\mu}) + \epsilon_{11}\epsilon_{33}\delta_{i3} \\ \times(\delta_{j1} + \delta_{j2})(p'_{44}u_{ji}^{\mu} + p'_{4\bar{4}}u_{ij}^{\mu}). \end{aligned} \tag{17}$$

Utilizing the Fourier transform of the displacement gradient $u_{ij}^{\mu}(\vec{r}, t)$, i.e., $u_{ij}^{\mu}(\vec{q}, t) = iqu^{\mu}(\vec{q}, t)\pi_i^{\mu}\kappa_j$, we obtain for the fluctuation of the electric displacement

$$\begin{aligned} \delta\vec{D}^{\mu}(\vec{q}, t) &= \delta\vec{\epsilon}^{\mu}(\vec{q}, t) \cdot \vec{E}_0 \\ &= (\epsilon_{11}^2/i)u^{\mu}(\vec{q}, t)qE_0\vec{\xi}^{\mu}, \end{aligned} \tag{18}$$

where

$$\begin{aligned} \vec{\xi}^{\mu} = &\sum_{i=1}^{3}\left[\sum_{m=1}^{3} p_{im}\left(\frac{\epsilon_{ii}}{\epsilon_{11}}\right)^2 \pi_m^{\mu}\kappa_m\right]E_{0,i}\vec{1}_i \\ &+ \tfrac{1}{2}(p_{11} - p_{12})(\pi_1^{\mu}\kappa_2 + \pi_2^{\mu}\kappa_1)(E_{0,2}\vec{1}_1 + E_{0,1}\vec{1}_2) \\ &+ \frac{\epsilon_{33}}{\epsilon_{11}} p'_{44}\kappa_3[\pi_1^{\mu}(E_{0,3}\vec{1}_1 + E_{0,1}\vec{1}_3) + \pi_2^{\mu}(E_{0,3}\vec{1}_2 + E_{0,2}\vec{1}_3)] \\ &+ \frac{\epsilon_{33}}{\epsilon_{11}} p'_{4\bar{4}}\pi_3^{\mu}[\kappa_1(E_{0,3}\vec{1}_1 + E_{0,1}\vec{1}_3) + \kappa_2(E_{0,3}\vec{1}_2 + E_{0,2}\vec{1}_3)]. \end{aligned} \tag{19}$$

If the rotational effect can be neglected, i.e., $p'_{44} = p'_{4\bar{4}} = p_{44}$, Eq. (19) is reduced to

$$\begin{aligned} \vec{\xi}^{\mu} = &\frac{p_{44}}{\epsilon_{11}^2}[(\vec{\epsilon}\cdot\hat{\pi}^{\mu})(\hat{E}_0\cdot\vec{\epsilon}\cdot\hat{\kappa}) + (\vec{\epsilon}\cdot\hat{\kappa})(\hat{E}_0\cdot\vec{\epsilon}\cdot\hat{\pi}^{\mu})] - \frac{2p_{44}}{\epsilon_{11}^2} \\ &\times\sum_{i=1}^{3}\epsilon_{ii}^2\pi_i^{\mu}\kappa_i E_{0,i}\vec{1}_i + \sum_{m=1}^{3}\left[\sum_{n=1}^{3} p_{mn}\left(\frac{\epsilon_{mm}}{\epsilon_{11}}\right)^2 \pi_n^{\mu}\kappa_n\right]E_{0,m}\vec{1}_m \\ &+ [\tfrac{1}{2}(p_{11} - p_{12}) - p_{44}][(\pi_1^{\mu}\kappa_2 + \pi_2^{\mu}\kappa_1)(E_{0,1}\vec{1}_2 + E_{0,2}\vec{1}_1)], \end{aligned} \tag{20}$$

in agreement with the results obtained by Hamaguchi.[33] In Eqs. (19) and (20) $\hat{\pi}^{\mu}$ is a unit vector tor in the direction of the polarization of the sound wave, $\hat{\kappa}$ is a unit vector in the direction of the acoustic-wave vector, $\hat{E}_0$ is a unit vector in the direction of polarization of the incident light, and $\vec{1}_i$ $(i = 1, 2, 3)$ are unit vectors along the cube axes. The components of $\hat{\pi}^{\mu}$, $\hat{\kappa}$, and $\hat{E}_0$ along these axes are π_i^{μ}, κ_i, and $E_{0,i}$. It appears from Eq. (3) that in a light scattering experiment the polarization direction of light scattered from the acoustic mode μ is given by the vector

$$\vec{\Xi}^{\mu} = \hat{k}_d \times (\hat{k}_d \times \vec{\xi}^{\mu}). \tag{21}$$

Thus, we observe the component of the fluctuation in $\delta\vec{D}^{\mu}(\vec{q}, t)$ which lies in a plane perpendicular to the direction of the scattered wave.

Taking into account the quantum-mechanical features of the lattice vibrations one must make the following replacements for the squared Fourier amplitude of the displacement[45]:

$$|u_{+}^{\mu}(\vec{q})|^2 \to |\langle n+1|u_{+}^{\mu}(\vec{q})|n\rangle|^2 = \frac{V}{(2\pi)^3}\frac{\hbar\Omega^{\mu}(\vec{q})[N^{\mu}(\vec{q})+1]}{2\rho[\Omega^{\mu}(\vec{q})]^2} \tag{22}$$

and

$$|u_{-}^{\mu}(q)|^2 \to |\langle n-1|u_{-}^{\mu}(\vec{q})|n\rangle|^2 = \frac{V}{(2\pi)^3}\frac{\hbar\Omega^{\mu}(\vec{q})N^{\mu}(\vec{q})}{2\rho[\Omega^{\mu}(\vec{q})]^2}, \tag{23}$$

where the plus sign corresponds to the Stokes component (phonon creation) and the minus sign to the anti-Stokes component (phonon annihilation). The volume of the solid is V and the density ρ. The occupation number of the phonons having wave vector $\vec{q}$ and polarization index μ is $N^{\mu}(\vec{q})$.

The intensity of light scattered from a thermal-equilibrium distribution of acoustic phonons can be found by combining Eqs. (3), (10), (18), and (21)–(23) remembering the orthogonality of the acoustic modes:

$$\begin{aligned} dI_{sc}(\vec{q}, \vec{R}) = \frac{c_d E_0^2}{8\pi}\left(\frac{\omega_i}{c}\right)^4 \frac{V}{(4\pi)^2}\epsilon_{11}^4 \sum_{i=1}^{3}\left(\epsilon_{ii}\sum_{\mu}\frac{(\Xi_i^{\mu})^2}{2\rho(V_p^{\mu})^2}\hbar\Omega^{\mu}(\vec{q})\right. \\ \left.\times\{[\langle n^{\mu}(\vec{q})\rangle + 1] + \langle n^{\mu}(\vec{q})\rangle\}\, d\Omega\right), \end{aligned} \tag{24}$$

where

$$\langle n^{\mu}(\vec{q})\rangle = \frac{1}{e^{\hbar\Omega^{\mu}(\vec{q})/k_B T} - 1} \tag{25}$$

is the mean occupation number of the phonons. For microwave phonons at room temperature one has $\hbar\Omega^{\mu}/k_B T \approx 10^{-3} - 10^{-5} \ll 1$ or, equivalently, $\langle n^{\mu}\rangle \approx k_B T/\hbar\Omega^{\mu} \gg 1$, showing that the Stokes and anti-Stokes components are equal in intensity, provided that $\vec{\Xi}^{\mu}$ is the same for the two components. This will be shown in Sec. III. Thus, if $\hbar\Omega^{\mu} \ll k_B T$, the intensity of light scattered from a certain nonequilibrium acoustic mode through a Stokes or anti-Stokes process into the solid angle $d\Omega$ during the optical pathlength db is given by

$$dI_{sc} = aI_0\frac{\pi^2 n_o^8}{\lambda_0^4}N^{\mu}(\vec{q})\hbar\Omega^{\mu}(\vec{q})\frac{\sum_{i=1}^{3}\epsilon_{ii}(\Xi_i^{\mu})^2}{2\rho(V_p^{\mu})^2}db\, d\Omega, \tag{26}$$

assuming $V = 1$. The quantity a is defined through $a = (c_d/c_i)(E_0^2/\sum_{j=1}^{3}\epsilon_{ij}|E_{0,j}|^2)$, where c_i is the phase

velocity of the incident beam. The component of the incident light intensity along $\vec{k}_i$ is denoted by $I_0 = (c_i/8\pi)\sum_{j=1}^{3}\epsilon_{jj}|E_{0,j}|^2$. Finally, the Brillouin-scattering cross section σ_B defined as the scattering efficiency per unit length per unit solid angle becomes

$$\sigma_B = \frac{a\pi^2 n_o^8}{\lambda_0^4} N_R^{\mu}(\vec{q}) k_B T \frac{\sum_{i=1}^{3}\epsilon_{ij}(\Xi_i^{\mu})^2}{2\rho(V_p^{\mu})^2}, \tag{27}$$

where $N_R^{\mu}(\vec{q})$ is the number of phonons in the mode $(\mu, \vec{q})$ measured relative to the number in thermal equilibrium. To evaluate the number of phonons in a certain mode from a Brillouin-scattering experiment one has to calculate a $\sum_{i=1}^{3}\epsilon_{ij}(\Xi_i^{\mu})^2/\rho(V_p^{\mu})^2$ for the conditions appropriate to one's experiment.

III. BRILLOUIN-SCATTERING CROSS SECTIONS OF ON-AXIS AND OFF-AXIS PHONONS IN CdS

The following discussion is intended to evaluate anisotropic Brillouin-scattering cross sections of T_1, T_2, and L phonons in CdS for some important scattering configurations. The treatment is based on the general theory derived in Sec. II. The acoustic wave propagates in an arbitrary crystallographic direction characterized by the off-axis angle θ. Owing to the crystal symmetry the discussion can be limited to the angular range $0 \le \theta \le \pi/2$. The scattering plane contains the c axis as shown in Fig. 1, and the incident light is polarized either perpendicular or parallel to this plane. For $\theta = \pi/2$, we also consider the case where the scattering plane coincides with the basal plane.

Since the optical anisotropy at the wavelength used, $\lambda_0 = 6328$ Å, is quite small in CdS, $(n_e - n_o)/\frac{1}{2}(n_e + n_o) \approx 6.9\times10^{-3}$, the difference of the directions of the Poynting vector and the wave vector of the scattered light can be neglected. Consequently, the scattering cross section is proportional to $|\vec{\Xi}^{\mu}|^2/\rho(V_p^{\mu})^2$. The angular dependence of the phase velocities for the three acoustic modes are calculated in the Appendix. The frequency dependence of V_p^{μ} is negligible for phonons detectable by Brillouin scattering with visible light. The direction-dependent piezoelectric stiffening of V_p^{μ} in insulating crystals is neglected here, but is taken into account in a separate paper concerning the contribution from the indirect photoelastic effect to the anisotropic Brillouin-scattering cross section in piezoelectric hexagonal crystals.[42] The present analysis is further simplified because the rotational contribution to the scattering cross section is quite small in CdS. Thus,

$$\frac{|p'_{44} - p'_{44}|}{|p'_{44} + p'_{44}|} = \frac{n_o^{-2} - n_e^{-2}}{2|p_{44}|} \approx 0.02$$

at $\lambda_0 = 6328$ Å if the measured value[11] of $|p_{44}|$ is used in the denominator.

Since the signs of the symmetric components of the photoelastic tensor appear to be unknown,[10,11] we must evaluate a Brillouin-scattering cross section corresponding to each of the sign combinations of the appropriate photoelastic constants.

Knowing α and β, i.e., the directions of the incident and scattered photons (see Fig. 1) for an absorption process, a symmetry consideration shows that the scattering kinematics for the corresponding emission process [same acoustic mode $(\mu, \vec{q})$ and same incident-light polarization] is obtained by the transformations $\alpha + \pi \to \alpha$ and $\beta + \pi \to \beta$.[32] Thus, $\hat{\kappa} \to \hat{\kappa}$, $\hat{\pi}^{\mu} \to \hat{\pi}^{\mu}$, and $\hat{E}_0 \to -\hat{E}_0$, implying $\vec{\xi}^{\mu} \to -\vec{\xi}^{\mu}$. Finally, since $\hat{k}_d \to -\hat{k}_d$ one obtains $\vec{\Xi}^{\mu} \to -\vec{\Xi}^{\mu}$. The last transformation shows that the Brillouin-scattering cross sections for an absorption process and the corresponding emission process are the same. In the following we consider absorption processes only.

A. Scattering on T_1 phonons

With the scattering plane containing the c axis two cases may be considered: (i) The polarization of the incident light is perpendicular to the scattering plane, and (ii) the polarization is parallel to this plane.

(i). $\hat{\kappa} = (\kappa_1, 0, \kappa_3)$, $\hat{\pi}^{T_1} = (0, 1, 0)$, $\hat{E}_0 = (0, 1, 0)$, and $\hat{k}_d = (k_{d,1}, 0, k_{d,3})$. In this case Eq. (19) is reduced to

$$\vec{\xi}^{T_1}_{\hat{e}\parallel\hat{s}} = p_{66}\kappa_1 \vec{1}_1 + (\epsilon_{33}/\epsilon_{11})p'_{44}\kappa_3 \vec{1}_3, \tag{28}$$

where $p_{66} = \frac{1}{2}(p_{11} - p_{12})$. The subscript $\hat{e} \parallel \hat{s}$ indicates that the incident-light polarization $(\hat{e} = \hat{E}_0)$ is parallel to the normal $(\hat{s})$ to the scattering plane. Substituting Eq. (28) into Eq. (21) one obtains

$$\vec{\Xi}^{T_1}_{\hat{e}\parallel\hat{s}} = [p_{66}\kappa_1 k_{d,3} - (\epsilon_{33}/\epsilon_{11})p'_{44}\kappa_3 k_{d,1}](k_{d,1}\vec{1}_3 - k_{d,3}\vec{1}_1). \tag{29}$$

From Eq. (29) it appears that the scattered light is polarized perpendicular to the incident beam. Defining θ as the angle between the acoustic-wave vector and the c axis, we obtain using Eq. (A6) and the relations $\hat{\kappa} = (\sin\theta, 0, \cos\theta)$ and $\hat{k}_d = (-\cos\beta, 0, \sin\beta)$

$$\frac{|\vec{\Xi}^{T_1}_{\hat{e}\parallel\hat{s}}|^2}{\rho(V_p^{T_1})^2} = \frac{[p_{66}\sin\theta\sin\beta + (\epsilon_{33}/\epsilon_{11})p'_{44}\cos\theta\cos\beta]^2}{c_{66}\sin^2\theta + c_{44}\cos^2\theta}, \tag{30}$$

where $c_{66} = \frac{1}{2}(c_{11} - c_{12})$. For a polarization rotation $\eta = \pi/2$, the refractive indices are $n_i = n_o$ and $n_d = n_e n_o (n_o^2\cos^2\beta + n_e^2\sin^2\beta)^{-1/2}$. Inserting these expressions in Eq. (9) the possible values of β corresponding to a given phonon mode (f, θ) can be calculated. After this the Brillouin-scattering cross section can be evaluated from Eq. (30).

(ii). $\hat{\kappa} = (\kappa_1, 0, \kappa_3)$, $\hat{\pi}^{T_1} = (0, 1, 0)$, $\hat{E}_0 = (E_{0,1}, 0, E_{0,3})$, and $\hat{k}_d = (k_{d,1}, 0, k_{d,3})$. In this case we have

$$\vec{\xi}^{T_1}_{\hat{e}\perp\hat{s}} = [p_{66}\kappa_1 E_{0,1} + (\epsilon_{33}/\epsilon_{11})p'_{44}\kappa_3 E_{0,3}]\vec{1}_2 = -\vec{\Xi}^{T_1}_{\hat{e}\perp\hat{s}}, \tag{31}$$

showing that $\eta = \pi/2$. From a Brillouin-scattering

kinematics analysis,[32] one finds that the components of $\hat{E}_0$ in case (i) are related to the components of $\hat{k}_d$ in case (ii) by $E_{0,1} = -k_{d,3}$ and $E_{0,3} = k_{d,1}$. Consequently, the Brillouin-scattering cross sections of cases (i) and (ii) are equal. The above consideration implies that Eqs. (4.8) and (4.10) in the paper of Hamaguchi[33] are identical.

In Figs. 2–8 are plotted a normalized Brillouin-scattering cross section of the T_1 phonon in the scattering configurations of the cases (i) and (ii), i.e.,

$$\Sigma_B^{T_1}(f,\theta) \equiv \frac{2\lambda_0^4 c_{44}\sigma_B^{T_1}}{\pi^2 n_o^6 n_e^4 (p'_{44})^2 N_R^{T_1}(\vec{q}) k_B T a} = \frac{[(\epsilon_{11}/\epsilon_{33})(p_{66}/p'_{44})\sin\theta\sin\beta + \cos\theta\cos\beta]^2}{(c_{66}/c_{44})\sin^2\theta + \cos^2\theta}, \tag{32}$$

as a function of the phonon frequency for different off-axis angles. In the above equation and throughout the rest of the work we have used the condensed notation $\Sigma_B^{T_1}$ for $\Sigma_{B,\hat{e}\parallel\hat{s}}^{T_1} = \Sigma_{B,\hat{e}\perp\hat{s}}^{T_1}$. Experimentally obtained numerical values of the photoelastic tensor elements have been reported by Maloney *et al.*[10] and by Dixon.[11] From the data of Maloney *et al.*,[10]

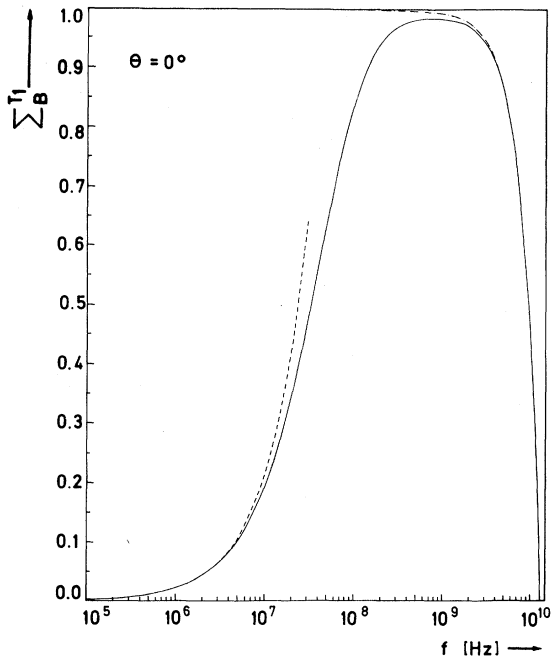

FIG. 2. Normalized Brillouin-scattering cross section $\Sigma_B^{T_1}$ for a T_1 phonon propagating along the c axis ($\theta = 0°$) as a function of the phonon frequency (f). The scattering geometry is shown in Fig. 1. The incident light is polarized either parallel or perpendicular to the scattering plane. The dashed and dot-dashed lines represent the analytical low- and high-frequency approximations to the cross section. (CdS, 300 K, $\lambda_0 = 6328$ Å.)

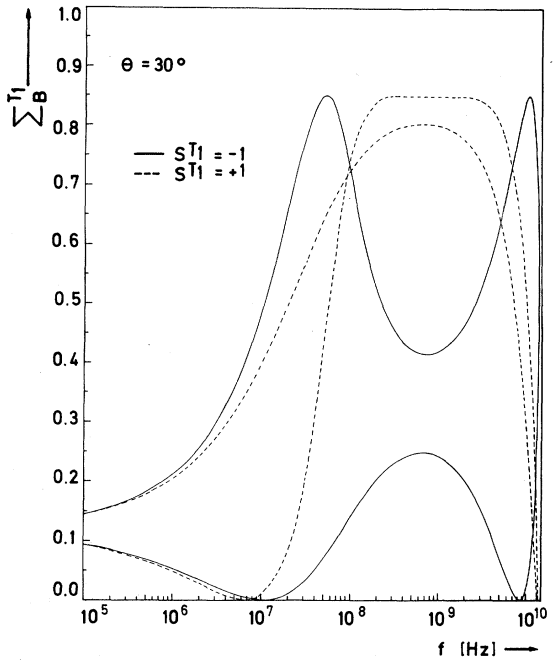

FIG. 3. Normalized Brillouin-scattering cross section $\Sigma_B^{T_1}$ for a T_1 phonon having an off-axis angle $\theta = 30°$ as a function of the phonon frequency (f). The cross section is plotted for the two possible sign combinations of the involved photoelastic constants, i.e., $S^{T_1} = p'_{44}p_{66}/|p'_{44}p_{66}| = \pm 1$. (CdS, 300 K, $\lambda_0 = 6328$ Å.)

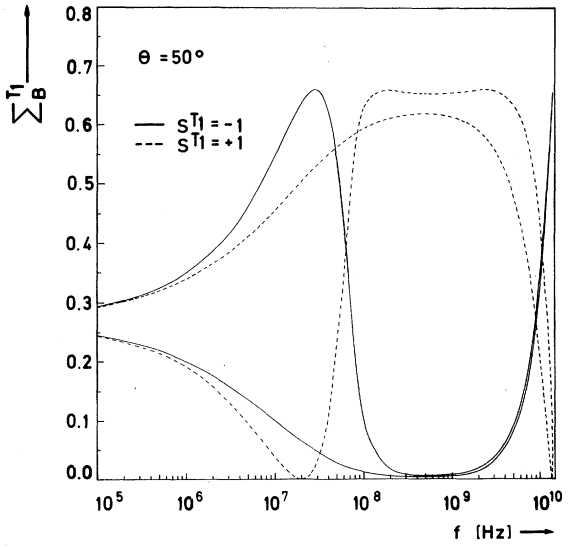

FIG. 4. Normalized Brillouin-scattering cross section $\Sigma_B^{T_1}$ for a T_1 phonon propagating in the direction $\theta = 50°$ as a function of the phonon frequency (f) for the two sign combinations $S^{T_1} = p'_{44}p_{66}/|p'_{44}p_{66}| = \pm 1$. Assuming $S^{T_1} = -1$ one finds $\Sigma_B^{T_1} \neq 0$ for all f. (CdS, 300 K, $\lambda_0 = 6328$ Å.)

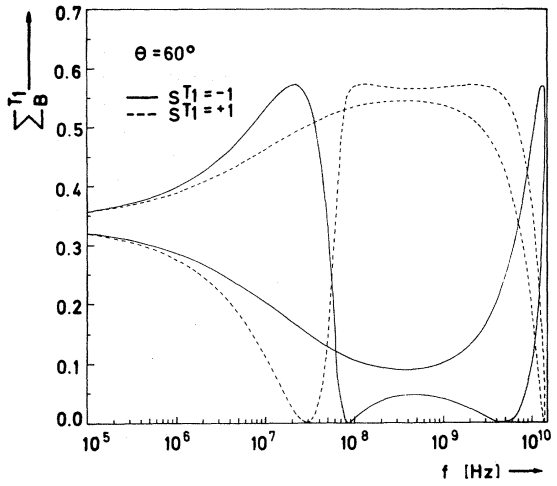

FIG. 5. Normalized Brillouin-scattering cross section $\Sigma_B^{T_1}$ for a T_1 phonon with an off-axis angle $\theta = 60°$ as a function of the phonon frequency (f) for the sign combinations $S^{T_1} = p'_{44}p_{66}/|p'_{44}p_{66}| = \pm 1$. (CdS, 300 K, $\lambda_0 = 6328$ Å.)

i.e., $|p_{66}| = \frac{1}{2}|p_{11} - p_{12}| \approx 0.032$, $|p_{11}| \approx 0.11$, and $|p_{12}| \approx 0.051$, it appears that p_{11} and p_{12} must have the same sign. Knowing this $\Sigma_B^{T_1}$ has been calculated on basis of the more accurate data of Dixon,[11] that is, $|p_{66}| = \frac{1}{2}|p_{11} - p_{12}| \approx \frac{1}{2}(0.142 - 0.066) = 0.038$ and $|p'_{44}| \approx |p_{44}| \approx 0.054$.

Utilizing the approximation $n_e - n_o \ll n_o$ in the anisotropic Bragg equation[32] (9) the normalized Brillouin-scattering cross section for phonons propagating along the c axis simplifies to

$$\Sigma_B^{T_1}(f, \theta = 0) = 1 - \left(\frac{\lambda}{\Lambda(0)\Delta}\right)^2 \left\{2 + \Delta + \left(\frac{\Lambda(0)\Delta}{\lambda}\right)^2 - 2\left[1 + \Delta + \left(\frac{\Lambda(0)\Delta}{\lambda}\right)^2\right]^{1/2}\right\}, \quad (33)$$

where $\Lambda(0) = V_p^{T_1}(0)/f$ is the acoustic wavelength along c and $\lambda \approx \lambda_0/n_i \approx \lambda_0/n_d$ is the optical wavelength inside the crystal. The optical anisotropy is given by the quantity $\Delta = 1 - (n_o/n_e)^2$. For low phonon frequencies $\Sigma_B^{T_1}$ is proportional to f, i.e., $\Sigma_B^{T_1}(f, \theta = 0) \approx 2\lambda f/\Delta\, V_p^{T_1}(0)$, and in the limit $f \to 0$, one has $\Sigma_B^{T_1} = 0$. For high frequencies one obtains $\Sigma_B^{T_1}(f, \theta = 0) \approx 1 - [\lambda f/2V_p^{T_1}(0)]^2$, that is, f^2 decrease in $\Sigma_B^{T_1}$. In the high-frequency limit $\Lambda(0) \to \lambda/2$ one gets $\Sigma_B^{T_1} = 0$. In Fig. 2 is shown $\Sigma_B^{T_1} = \Sigma_B^{T_1}(f, \theta = 0)$ together with the high- and low-frequency approximations to $\Sigma_B^{T_1}$. Note that the T_1 and T_2 modes are degenerated along the c axis.

For $\theta = \pi/2$ there are two nonequivalent possibilities for the scattering kinematics.[32] Consequently, $\Sigma_B^{T_1}(f, \theta = \pi/2)$ has two branches. With the approximation $n_e - n_o \ll n_o$ the normalized Brillouin-scattering cross section for the nearly isotropic Bragg kinematics[32] can be found by using Eqs. (9) and (32):

$$\Sigma_B^{T_1,\mathrm{iso}}(f, \theta = \pi/2) = \left(\frac{\epsilon_{11}}{\epsilon_{33}}\right)^2 \left(\frac{p_{66}}{p'_{44}}\right)^2 \frac{c_{44}}{c_{66}} \left[1 - \left(\frac{\lambda}{2\Lambda(\pi/2)}\right)^2\right] \quad (34)$$

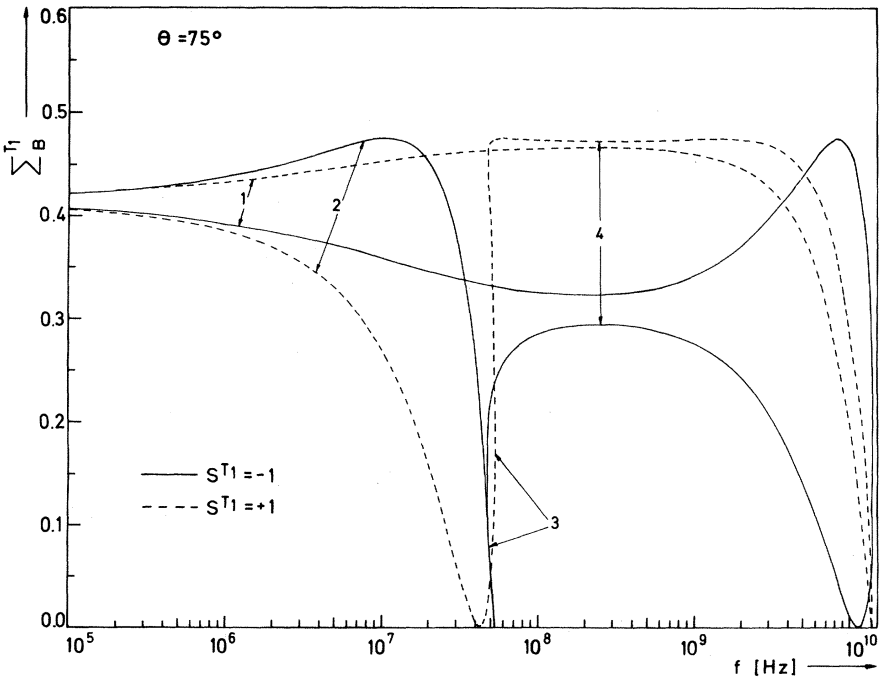

FIG. 6. Normalized Brillouin-scattering cross section $\Sigma_B^{T_1}$ for a T_1 phonon with an off-axis angle $\theta = 75°$ as a function of the phonon frequency (f) for the two sign combinations $S^{T_1} = p'_{44}p_{66}/|p'_{44}p_{66}| = \pm 1$. The numbers attached to the branches of $\Sigma_B^{T_1}$ assign these to the different nonequivalent scattering geometries discussed in Ref. 32. (CdS, 300 K, $\lambda_0 = 6328$ Å.)

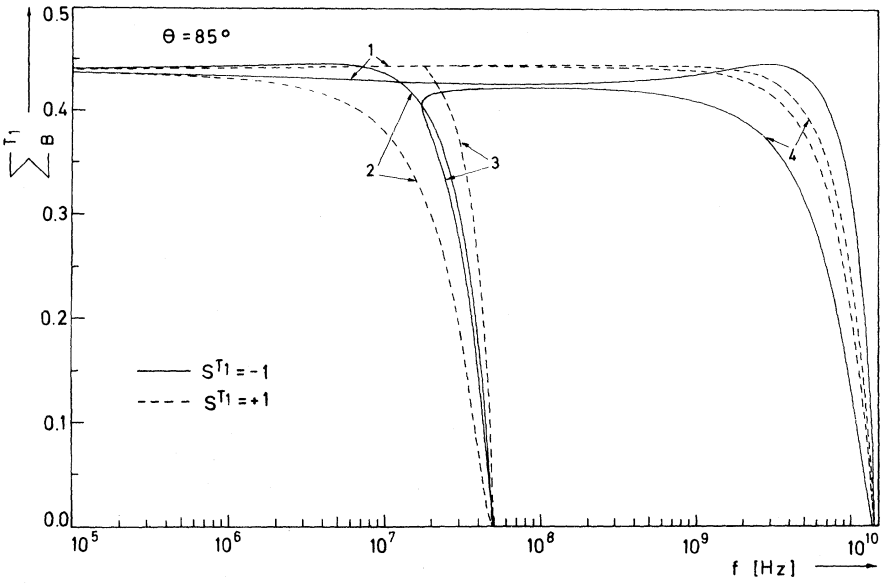

FIG. 7. Normalized Brillouin-scattering cross section $\Sigma_B^{T_1}$ for a T_1 phonon propagating in the direction $\theta = 85°$ as a function of the phonon frequency (f) for the two sign combinations $S^{T_1} = p'_{44}p'_{66}/|p'_{44}p'_{66}| = \pm 1$. The numbers attached to the branches of $\Sigma_B^{T_1}$ assign these to the different nonequivalent scattering geometries discussed in Ref. 32. Note that there are four different cross sections in a certain range of phonon frequencies. (Cds, 300 K, $\lambda_0 = 6328$ Å.)

The nearly isotropic case has an upper cutoff frequency $f = (n_e + n_o)\, V_p^{T_1}(\pi/2)/\lambda_0$. In the limit $\Lambda(\pi/2) \to \lambda/2$, $\Sigma_B^{T_1,\mathrm{iso}} \to 0$. For the highly anisotropic branch,[32] having an upper cutoff frequency at $f = (n_e - n_o)V_p^{T_1}(\pi/2)/\lambda_0$, the normalized Brillouin-scattering cross section is

$$\Sigma_B^{T_1,\mathrm{aniso}}(f, \theta = \pi/2) = \left(\frac{\epsilon_{11}}{\epsilon_{33}}\right)^2 \left(\frac{p_{66}}{p'_{44}}\right)^2 \frac{c_{44}}{c_{66}} \left[1 - \left(\frac{2\lambda}{\Lambda(\pi/2)\Delta}\right)^2\right], \tag{35}$$

as can be shown by combining Eqs. (9) and (32). For this branch $\Sigma_B^{T_1,\mathrm{aniso}} \to 0$ for $\Lambda(\pi/2) \to 2\lambda/\Delta$. In Fig. 8 is shown the frequency dependence of the normalized Brillouin-scattering cross sections for $\theta = \pi/2$. Note that $\Sigma_B^{T_1,\mathrm{iso}}$ and $\Sigma_B^{T_1,\mathrm{aniso}}$ are essentially independent of the phonon frequency for $f \lesssim 1$ GHz and $f \lesssim 1$ MHz, respectively. For $\theta = 0$, $\pi/2$ the phonon frequencies for which the cross section vanishes coincide with the frequencies for which the diffraction process is collinear with a scattering angle $\Phi_s = 0$ or π.[32]

For $\theta \neq 0, \pi/2$ a Brillouin-scattering cross section must be evaluated for each of the two possibilities $S^{T_1} = p'_{44}p_{66}/|p'_{44}p_{66}| = \pm 1$.

In Figs. 3–7 is shown the normalized Brillouin-scattering cross section as a function of the phonon

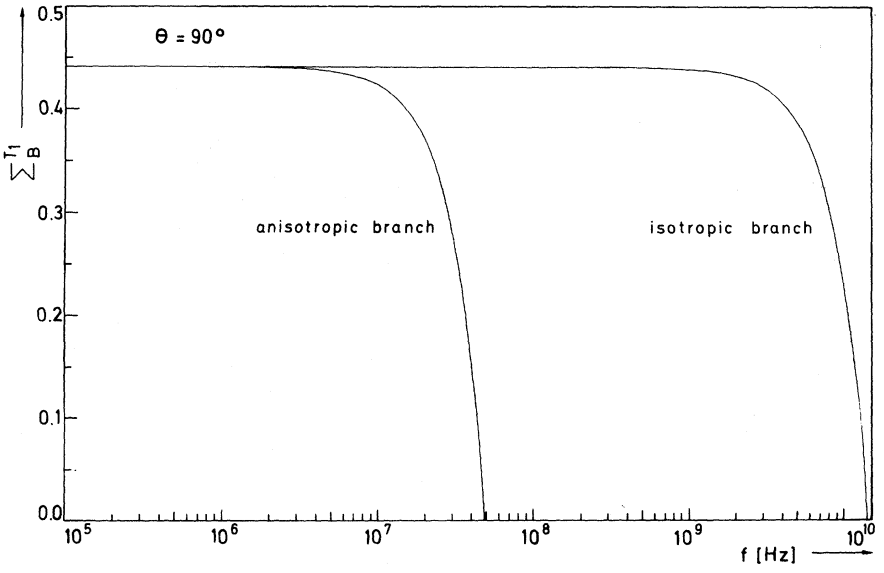

Fig. 8. Normalized Brillouin-scattering cross section $\Sigma_B^{T_1}$ for a phonon propagating perpendicular to the optic axis ($\theta = 90°$) as a function of the phonon frequency (f). The scattering geometry is shown in Fig. 1. Note that the cross section has a nearly isotropic branch and a highly anisotropic branch. (CdS, 300 K, $\lambda_0 = 6328$ Å.)

frequency for $\theta = 30°$, 50°, 60°, 75°, and 85°. In the low-frequency limit one has[32] $\beta \to \pi/2$, implying

$$\Sigma_B^{T_1}(f \to 0, \theta) = \left(\frac{\epsilon_{11}}{\epsilon_{33}}\right)^2 \left(\frac{p_{66}}{p'_{44}}\right)^2 \frac{1}{c_{66}/c_{44} + \cot^2\theta} \,. \tag{36}$$

Thus, for low frequencies $\Sigma_B^{T_1}$ is independent of S^{T_1}, and increases with increasing θ. In the high-frequency limit, i.e., for $\Lambda(\theta) \to \lambda/2$, we obtain

$$\Sigma_B^{T_1}(\Lambda \to \lambda/2, \theta) = \tfrac{1}{4}\left(1 - \frac{\epsilon_{11}}{\epsilon_{33}} \frac{p_{66}}{p'_{44}}\right)^2 \sin^2\theta. \tag{37}$$

According to Eq. (37) the Brillouin-scattering cross section equals zero at the upper cutoff frequency for $\theta = 0$ and $\pi/2$ only. In the limit $\Lambda(\theta) \to \lambda/2$ the ratio of the scattering cross sections corresponding to $S_1^T = +1$ and -1 is

$$\frac{[1 - (\epsilon_{11}/\epsilon_{33}) \mid p_{66}/p'_{44}\mid]^2}{[1 + (\epsilon_{11}/\epsilon_{33}) \mid p_{66}/p'_{44}\mid]^2} \approx 0.033$$

for $\theta \neq 0$ and $\pi/2$.

A study of the scattering kinematics for the T_1 phonon[32] shows that there are two non-equivalent scattering geometries in the angular range $0° < \theta \lesssim 72.5°$. Consequently, we obtain two different scattering cross sections for a given phonon frequency (see Figs. 3–5). In the range $72.5° \lesssim \theta < 90°$ there are four nonequivalent scattering geometries in a certain range of phonon frequencies.[32] The extension of the frequency range depends on θ. Examples of Brillouin-scattering cross sections exhibiting four branches are shown in Figs. 6 and 7. The number attached to the branches of $\Sigma_B^{T_1}(f, \theta)$ assign these to the different nonequivalent scattering geometries discussed in Ref. 32.

The phonon frequencies for which the cross section $\Sigma_B^{T_1} = 0$ depend on the phonon off-axis angle and can be evaluated by substituting the value of β found from the relation

$$\tan\beta = -\frac{\epsilon_{33}}{\epsilon_{11}} \frac{p'_{44}}{p_{66}} \cot\theta, \quad \left(\left|\vec{\Xi}^{T_1}_{\vec{e}\|\vec{s}}\right| = 0\right)$$

into the anisotropic Bragg equation (9) and by solving this with respect to f. In Fig. 9 is shown $f = f(\theta)$ for $\Sigma_B^{T_1} = 0$. For $\theta \to 0$ one obtains $f \to 0$ or $2n_o V_p^{T_1}(0)/\lambda_0$, and for $\theta \to \pi/2$, f approximates $(n_e - n_o)V_p^{T_1}(\pi/2)/\lambda_0$ or $(n_e + n_o)V_p^{T_1}(\pi/2)\,\lambda_0$. Supposing $S^{T_1} = +1$, f increases monotonically with increasing θ in both branches. Assuming $S^{T_1} = -1$ there exists an angular gap $48.5° \lesssim \theta \lesssim 52.5°$, in which $\Sigma_B^{T_1} \neq 0$ for all f. Outside this gap one finds two zeros for a given θ. In Fig. 4 the frequency dependence of $\Sigma_B^{T_1}$ was calculated for an off-axis angle ($\theta = 50°$) within the gap. Note that $0 < \Sigma_B^{T_1}(f, \theta = 50°) \lesssim 0.01$ in the range $0.25 \lesssim f \lesssim 1.30$ GHz for $S^{T_1} = -1$. For $\theta \neq 0, \pi/2$ the phonon frequencies giving $\Sigma_B^{T_1} = 0$ do not coincide with the frequencies for which the scattering process is collinear.[32]

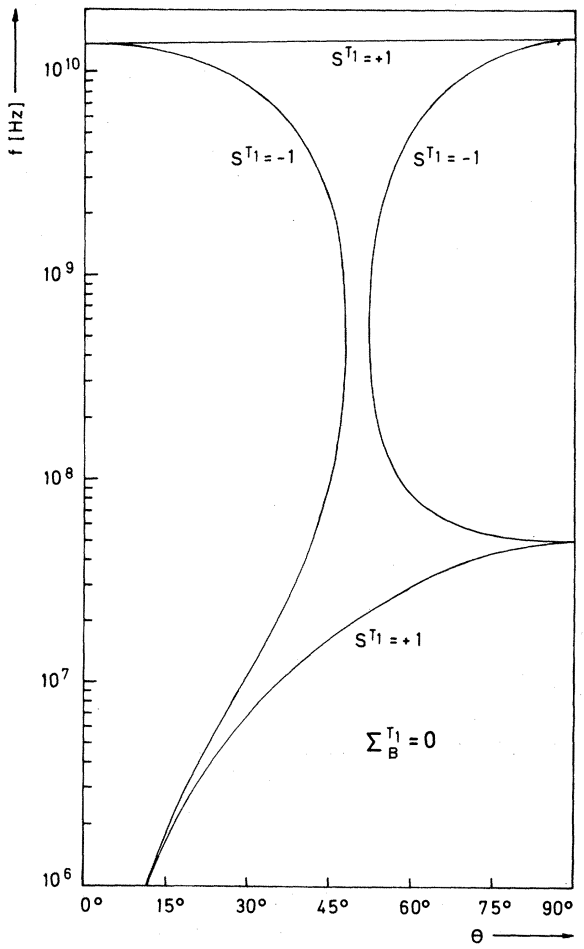

FIG. 9. Phonon frequencies (f) versus phonon off-axis angle (θ) for the T_1-phonon diffraction processes where the Brillouin-scattering cross section vanishes ($\Sigma_B^{T_1} = 0$). The scattering geometry is shown in Fig. 1. Curves are plotted for the two possible sign combinations, $S^{T_1} = p'_{44}p_{66}/\mid p'_{44}p_{66}\mid = \pm 1$. For $\theta \to 0$, f approaches 0 or $2n_o V_p^{T_1}(0)/\lambda_0$. Note the angular gap in which $\Sigma_B^{T_1} \neq 0$ if $S^{T_1} + -1$. (CdS, 300 K, $\lambda_0 = 6328$ Å).

The angular dependence of the normalized Brillouin-scattering cross section for the collinear diffraction processes is given by

$$\Sigma_B^{T_1}(f = f_c^{\pm}(\theta), \theta) = \frac{[(\epsilon_{11}/\epsilon_{33})(p_{66}/p'_{44}) - 1]^2 \sin^2 2\theta}{4[(c_{66}/c_{44})\sin^2\theta + \cos^2\theta]} \,, \tag{38}$$

as readily can be verified by substituting $\beta = \theta + \pi/2$ into Eq. (32). It appears from Eq. (38) that the angular dependences of the cross sections corresponding to scattering angles $\Phi_s = 0$ (minus sign) and $\Phi_s = \pi$ (plus sign) are identical. The angular variation of the scattering cross section for the collinear diffraction processes is shown on Fig. 10.

Being interested in the angular distribution of the collection of monochromatic acoustic waves in an

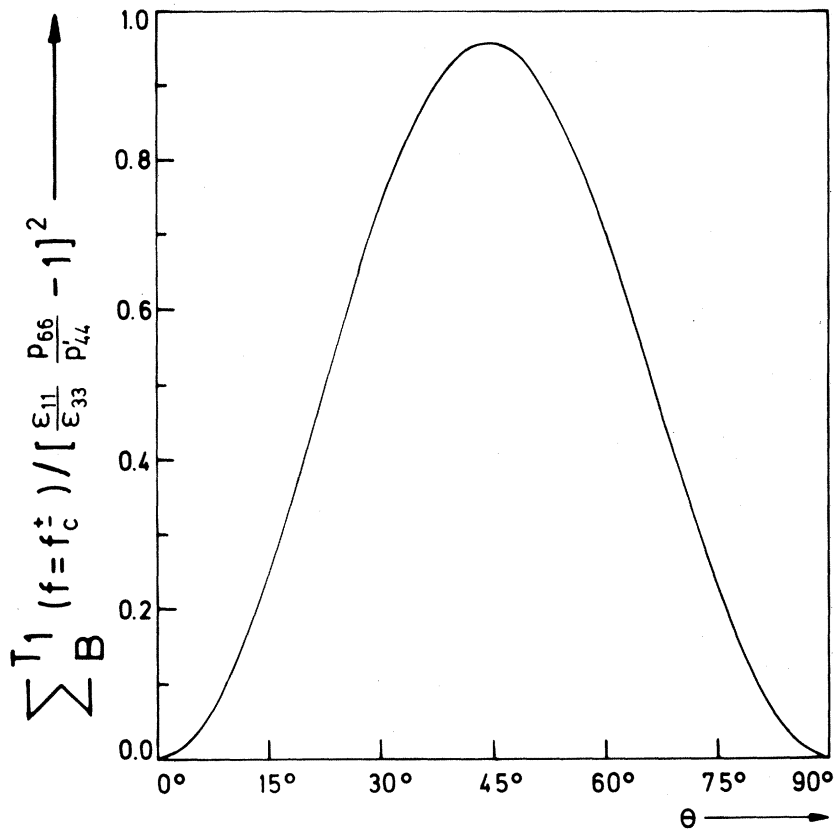

FIG. 10. Angular dependence of the normalized Brillouin-scattering cross section for the two collinear diffraction processes ($f=f_c^{\pm}$) for the T_1 phonon. Note that the cross section is independent of the scattering angle ($\Phi_s=0$ or π). (CdS, 300 K.)

acoustoelectrically inactive domain the scattering cross section must be plotted as a function of θ with f as a parameter. As illustrated in Fig. 11 the angular dependence of the cross section varies considerably with the phonon frequency.

Since the normalized scattering cross section of the T_1 mode depends strongly on S^{T1} in certain ranges of phonon frequencies and off-axis angles the relative signs of p_{44} and p_{66} can be obtained from a Brillouin-scattering experiment on an appropriate phonon mode (f, θ). The modes giving $\Sigma_B^{T1}=0$ for either $S^{T1}=+1$ or -1 should be especially suitable for this purpose.

When $\theta=\pi/2$ we may take the c plane as the scattering plane and consider the cases where the polarization of the incident light is either parallel (i) or perpendicular (ii) to c.

(i) $\hat{\kappa}=(1, 0, 0)$, $\hat{\pi}^{T1}=(0, 1, 0)$, $\hat{E}_0=(0, 0, 1)$, and $\hat{k}_d=(k_{d,1}, 0, k_{d,3})$. Using Eq. (19) one obtains

$$\vec{\xi}^{T_1}_{\hat{e}\parallel\hat{c}}=\vec{0}\,. \tag{39}$$

In the above subscript $\hat{c}$ is a unit vector parallel to the optic axis. Since the incident electric field produces no fluctuations in the electric displacement, there is no Brillouin scattering in this case.

(ii) $\hat{\kappa}=(1, 0, 0)$, $\hat{\pi}^{T1}=(0, 1, 0)$, $\hat{E}_0=(E_{0,1}, E_{0,2}, 0)$, and $\hat{k}_d=(k_{d,1}, k_{d,2}, 0)$. In this case Eq. (19) is reduced to

$$\vec{\xi}^{T_1}_{\hat{e}\perp\hat{c}}=p_{66}(E_{0,2}\vec{I}_1+E_{0,1}\vec{I}_2)\,. \tag{40}$$

Using Eq. (21) one finds a polarization rotation $\eta=0$. This implies that the pseudomomentum-conservation triangle is isosceles. Consequently, $k_{d,1}=E_{0,2}$ and $k_{d,2}=E_{0,1}$. Inserting these relations and Eq. (39) in Eq. (21) one finds

$$\vec{\Xi}^{T_1}_{\hat{e}\perp\hat{c}}=\vec{0}\,. \tag{41}$$

In this case there is no Brillouin scattering since the produced fluctuation in the electric displacement has no component perpendicular to the direction of the scattered wave.

B. Common features for T_2- and L-phonon scattering

When the scattering plane contains the c axis the incident light can be polarized either perpendicular (i) or parallel (ii) to this plane. In case (i) the diffraction configuration can be characterized as follows:

(i) $\hat{\kappa}=(\kappa_1, 0, \kappa_3)$, $\hat{\pi}^{\mu}=(\pi_1^{\mu}, 0, \pi_3^{\mu})$, $\hat{E}_0=(0, 1, 0)$, and $\hat{k}_d=(k_{d,1}, 0, k_{d,3})$, where $\mu=T_2$ or L. Using Eqs. (19) and (21) one obtains

$$\vec{\xi}^{\mu}_{\hat{e}\parallel\hat{s}}=(p_{12}\kappa_1\pi_1^{\mu}+p_{13}\kappa_3\pi_3^{\mu})\vec{I}_2=-\vec{\Xi}^{\mu}_{\hat{e}\parallel\hat{s}}\,. \tag{42}$$

Combining Eqs. (27) and (42) it follows that the Brillouin-scattering cross section for a thermal distribution of T_2 or L phonons is independent of

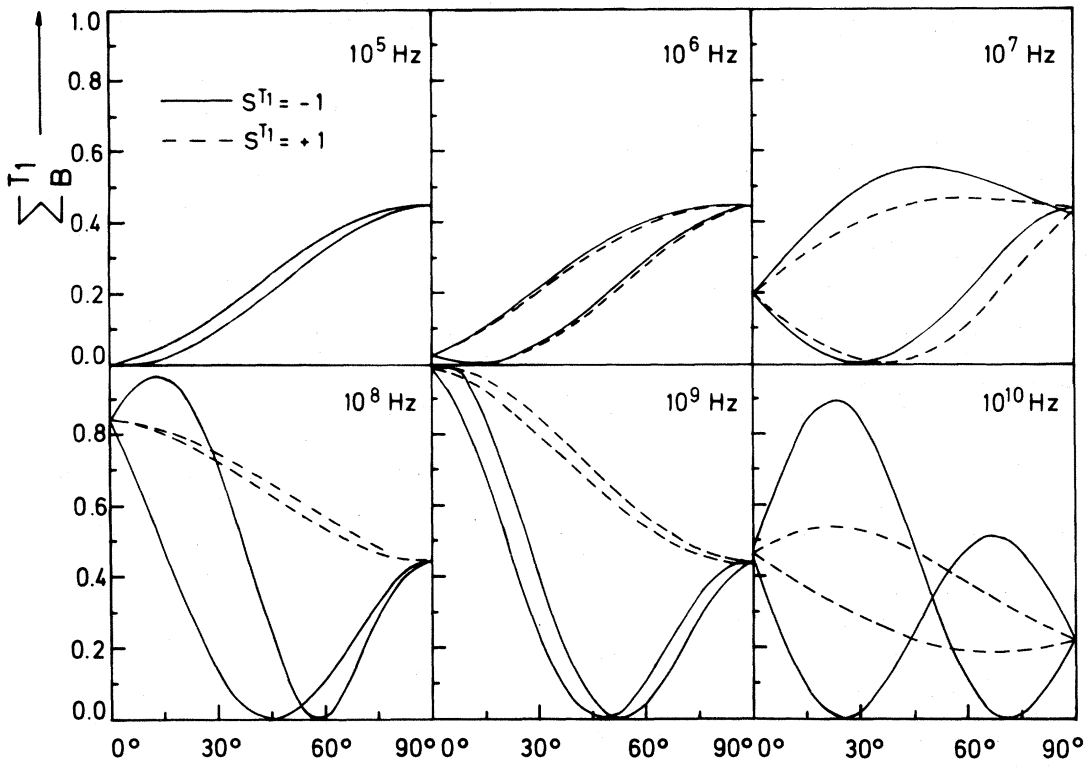

FIG. 11. Normalized Brillouin-scattering cross section for the T_1 phonon, $\Sigma_B^{T_1}$, as a function of the phonon off-axis angle (θ) for different phonon frequencies. Curves are plotted for the two possible sign combinations of the involved photoelastic tensor elements, i.e., $S^{T_1} = p'_{44}p_{66}/|p'_{44}p_{66}| = \pm 1$. (CdS, 300 K, $\lambda_0 = 6328$ Å.)

the phonon frequency in this case. The rotational effect does not contribute to the scattering cross section. Since the polarization rotation $\eta = 0$ the scattering kinematics is governed by the isotropic Bragg law ($n_i = n_d = n_o$).

In case (ii) the scattering kinematics is as follows:

(ii) $\hat{\kappa} = (\kappa_1, 0, \kappa_3)$, $\hat{\pi}^\mu = (\pi_1^\mu, 0, \pi_3^\mu)$, $\hat{E}_0 = (E_{0,1}, 0, E_{0,3})$, and $\hat{k}_d = (k_{d,1}, 0, k_{d,3})$. Utilizing Eqs. (19) and (21) one finds

$$\vec{\Xi}^\mu_{\hat{e}\parallel\hat{3}} = (k_{d,1}\xi_3^\mu - k_{d,3}\xi_1^\mu)(k_{d,3}\vec{1}_1 - k_{d,1}\vec{1}_3)\,, \tag{43}$$

where

$$\xi_1^\mu = (p_{11}\kappa_1\pi_1^\mu + p_{13}\kappa_3\pi_3^\mu)E_{0,1} + (\epsilon_{33}/\epsilon_{11})(p'_{44}\kappa_3\pi_1^\mu + p'_{44}\kappa_1\pi_3^\mu)E_{0,3} \tag{44}$$

and

$$\xi_3^\mu = (\epsilon_{33}/\epsilon_{11})^2(p_{31}\kappa_1\pi_1^\mu + p_{33}\kappa_3\pi_3^\mu)E_{0,3} + (\epsilon_{33}/\epsilon_{11})(p'_{44}\kappa_3\pi_1^\mu + p'_{44}\kappa_1\pi_3^\mu)E_{0,1} \tag{45}$$

are the nonvanishing components of the vector $\vec{\xi}^\mu$. According to Eq. (43) the polarization rotation is $\eta = 0$ for both the T_2 and L mode implying $n_i = n_e n_o \times (n_o^2\cos^2\alpha + n_e^2\sin^2\alpha)^{-1/2}$ and $n_d = n_e n_o(n_o^2\cos^2\beta + n_e^2 \times \sin^2\beta)^{-1/2}$. The quantity appropriate to a scattering experiment becomes $(\xi_1^\mu k_{d,3} - \xi_3^\mu k_{d,1})^2/\rho(V_p^\mu)^2$. Thus, in general the scattering cross section depends on both the phonon frequency and the off-axis angle, and since the signs of the symmetric photoelastic tensor elements are unknown one will, in principle, have to evaluate 16 possible Brillouin-scattering cross sections for an acoustic wave propagating in a general crystallographic direction.

C. Scattering on T_2 phonons

The polarization direction of an off-axis quasi-transverse phonon is determined by the unit vector

$$\hat{\pi}^{T2} = (\cos(\theta+\delta), 0, -\sin(\theta+\delta)) = ([A_{33} - (V_p^{T2})^2]/\{[[A_{33} - (V_p^{T2})^2]^2 + A_{13}^2\}^{1/2}, 0, A_{13}/\{[A_{33} - (V_p^{T2})^2]^2 + A_{13}^2\}^{1/2})\,,$$

where δ is the angular deviation of T_2 from a pure mode. The angular dependence of δ, A_{13}, A_{33}, and V_p^{T2} has been given in the Appendix. Combining Eqs. (27) and (42) yields the following normalized Brillouin scattering cross section for case (i) of Sec. III B:

$$\Sigma_{B,\hat{e}\parallel\hat{3}}^{T2}(\theta) \equiv \frac{2\lambda_0^4 c_{44}\sigma_{B,\hat{e}\parallel\hat{3}}^{T2}}{\pi^2 n_o^8 p_{13}^2 N_R^{T2}(\vec{q})k_B T}$$

$$= \frac{1}{4}\left(\frac{V_p^{T2}(0)}{V_p^{T2}(\theta)}\right)^2\left(\frac{p_{12}}{p_{13}}\frac{\cos(\theta+\delta)}{\cos\theta} - \frac{\sin(\theta+\delta)}{\sin\theta}\right)^2 \sin^2 2\theta. \tag{46}$$

For $\theta = 0$ or $\pi/2$ one has $\delta = 0$, implying $\Sigma^{T2}_{B,\hat{e}\parallel\hat{s}}(\theta = 0, \pi/2) = 0$. Neglecting the deviation δ, which is a fair approximation in CdS since $\delta(\theta)/\theta \lesssim 0.16$, the normalized cross section equals

$$\Sigma^{T2}_{B,\hat{e}\parallel\hat{s}}(\theta) = \frac{1}{4}\left(\frac{p_{12}}{p_{13}} - 1\right)^2 \left(\frac{V_p^{T2}(0)}{V_p^{T2}(\theta)}\right)^2 \sin^2 2\theta\ .$$

In Fig. 12 is shown $\Sigma^{T2}_{B,\hat{e}\parallel\hat{s}} = \Sigma^{T2}_{B,\hat{e}\parallel\hat{s}}(\theta)$ for the two possible sign combinations, $S_\perp^{T2} = p_{12}p_{13}/|p_{12}p_{13}| = \pm 1$, of the photoelastic constants. The numerical values $|p_{12}| \approx 0.051$ and $|p_{13}| \approx 0.072$, were taken from Ref. 10.

In case (ii) of Sec. III B the wave vectors of the incident and scattered light belong to the same shell of the index surface, which is an ellipsoid of revolution.[32,35] Since $n_e - n_o \ll n_o$ in CdS the ellipsoid can be approximated by a sphere of radius $n = (n_e n_o)^{1/2} \approx n_o \approx n_e$. Thus, replacing the anisotropic Bragg equations by the isotropic Bragg law one finds $\hat{E}_0 = (\sin(\theta - \Phi_B^{T2}), 0, \cos(\theta - \Phi_B^{T2}))$, and $\hat{k}_d = (-\cos(\theta + \Phi_B^{T2}), 0, \sin(\theta + \Phi_B^{T2}))$, where the Bragg angle in the isotropic case is given by $\Phi_B^{T2} = \arcsin[\lambda_0 f/2nV_p^{T2}(\theta)]$. Neglecting, furthermore, the deviation δ the normalized Brillouin-scattering cross section takes the form

$$\Sigma^{T2}_{B,\hat{e}\perp\hat{s}}(f,\theta) \equiv \frac{2\lambda_0^4 c_{44}\sigma^{T2}_{B,\hat{e}\perp\hat{s}}}{\pi^2 n^8 p_{44}^2 N_R^{T2}(\vec{q}) k_B T}$$

$$= \left(\frac{V_p^{T2}(0)}{V_p^{T2}(\theta)}\right)^2 \left[\left(1 - \frac{p_{31}-p_{33}}{2p_{44}}\right)\cos^2\theta - \left(1 + \frac{p_{11}-p_{13}}{2p_{44}}\right)\sin^2\theta + \frac{(p_{11}-p_{13})+(p_{31}-p_{33})}{2p_{44}}\left(\frac{\lambda_0}{2nV_p^{T2}(\theta)}\right)^2 f^2\right]^2 \sin^2 2\theta. \tag{47}$$

Since experimental values for the combinations of photoelastic constants $|p_{11}-p_{13}|$ and $|p_{31}-p_{33}|$ have been given by Maloney *et al.*,[10] the approximate expression for the normalized cross section needs to be evaluated numerically for four sign combinations only. If $\theta = 0$ or $\pi/2$, $\Sigma^{T2}_{B,\hat{e}\perp\hat{s}} = 0$, a result which also holds when $\Sigma^{T2}_{B,\hat{e}\perp\hat{s}}$ is calculated on the basis of Eqs. (27) and (43)–(45), since the Bragg triangle is isosceles in these cases.[32] In the low-frequency limit one obtains immediately from Eq. (47)

$$\Sigma^{T2}_{B,\hat{e}\perp\hat{s}}(f \to 0, \theta) = \left(\frac{V_p^{T2}(0)}{V_p^{T2}(\theta)}\right)^2 \left[\left(1 - \frac{(p_{31}-p_{33})}{2p_{44}}\right)\cos^2\theta - \left(1 + \frac{(p_{11}-p_{13})}{2p_{44}}\right)\sin^2\theta\right]^2 \sin^2 2\theta,$$

and in the high-frequency limit Eq. (47) is reduced to

$$\Sigma^{T2}_{B,\hat{e}\perp\hat{s}}(\Lambda(\theta) \to \lambda/2, \theta) = \left(\frac{V_p^{T2}(0)}{V_p^{T2}(\theta)}\right)^2 \left[\left(1 - \frac{(p_{11}-p_{13})}{2p_{44}}\right)\cos^2\theta - \left(1 - \frac{(p_{31}-p_{33})}{2p_{44}}\right)\sin^2\theta\right]^2 \sin^2 2\theta.$$

For $\theta = \pi/4$ the normalized cross section in Eq. (47) is reduced to the simple form

$$\Sigma^{T2}_{B,\hat{e}\perp\hat{s}}(f, \theta = \pi/4) = \left(\frac{V_p^{T2}(0)}{V_p^{T2}(\pi/4)}\right)^2 \times \left(\frac{p_{11}-p_{13}+p_{31}-p_{33}}{4p_{44}}\right)^2 \cos^2 2\Phi_B^{T2}. \tag{48}$$

In Fig. 13 is shown the normalized cross section of Eq. (48) reduced by the factor $[V_p^{T2}(0)/V_p^{T2}(\pi/4)]^2 \times [(p_{11}-p_{13}+p_{31}-p_{33})/4p_{44}]^2$ as a function of the phonon frequency. From Eq. (48) it is easily found that the cross section vanishes for $f = \sqrt{2}nV_p^{T2}(\pi/4)/\lambda_0 = f_{\max}^{T2}(\theta = \pi/4)/\sqrt{2}$, where $f_{\max}$ is the upper cutoff

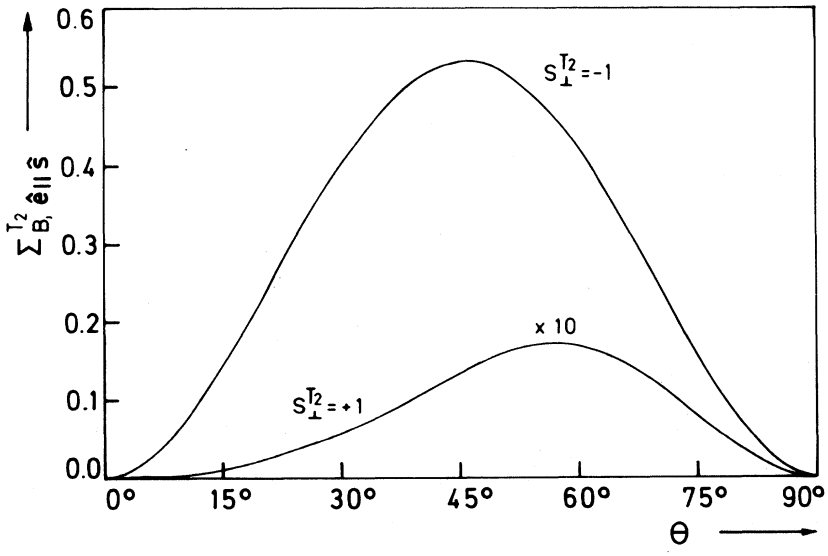

FIG. 12. Frequency-independent normalized Brillouin-scattering cross section $\Sigma^{T2}_{B,\hat{e}\parallel\hat{s}}$ for a T_2 phonon as a function of the phonon off-axis angle (θ). The incident photon is polarized perpendicular to the scattering plane which as shown in Fig. 1 contains the c axis. The cross section is plotted for the two possible sign combinations of the involved photoelastic tensor components, i.e., $S_\perp^{T2} = p_{12}p_{13}/|p_{12}p_{13}| = \pm 1$. The cross section corresponding to $S_\perp^{T2} = +1$ has been multiplied by a factor of 10. (CdS, 300 K, $\lambda_0 = 6328$ Å.)

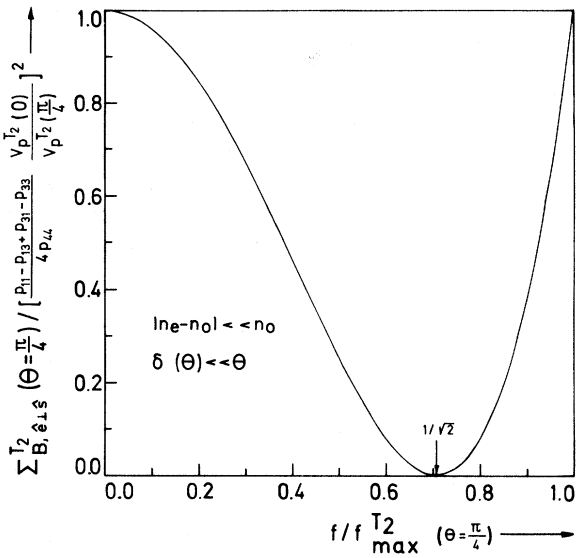

FIG. 13. Reduced Brillouin-scattering cross section $\Sigma^{T_2}_{B,\hat{e}\perp\hat{s}}/\{[(p_{11}-p_{13}+p_{31}-p_{33})/4p_{44}][V_p^{T_2}(0)/V_p^{T_2}(\pi/4)]\}^2$, for a T_2 phonon with an off-axis angle $\theta=\pi/4$ as a function of the reduced phonon frequency $f/f^{T_2}_{max}(\theta=\pi/4)$, in the limit of small optical anisotropy, i.e., $|n_e-n_o| \ll n_o$, and in the limit of small longitudinal admixture in the mixed T_2 mode, i.e., $\delta(\theta) \ll \theta$. With the incident photon polarized parallel to the scattering plane the diffraction kinematics is shown in Fig. 1.

frequency, and that it has two maxima of equal magnitude at $f=0$ and $f^{T_2}_{max}$.

Below we summarize, for completeness, the results obtained by Hamaguchi[33] for the case where $\theta=\pi/2$ and we take the basal plane as the scattering plane. The incident light can be polarized (i) in the c plane or (ii) parallel to the c axis.

(i) $\hat{\kappa}=(1,0,0)$, $\hat{\pi}^{T_2}=(0,0,1)$, $\hat{E}_0=(E_{0,1},E_{0,2},0)$, and $\hat{k}_d=(k_{d,1},k_{d,2},0)$. From the equation

$$\vec{I}^{T_2}_{\hat{e}\perp\hat{c}} = -(\epsilon_{33}/\epsilon_{11})p'_{44}E_{0,1}\vec{I}_3 , \tag{49}$$

we find that the scattered light is polarized perpendicular to the incident beam, i.e., $\eta=\pi/2$, so that $n_i=n_o$ and $n_d=n_e$. The scattering kinematics for the present case has been discussed by Dixon.[34] Note that p_{44} in Eq. (4.2) of Hamaguchi's paper[33] is replaced by p'_{44} if we take the rotational effect into account.

(ii) $\hat{\kappa}=(1,0,0)$, $\hat{\pi}^{T_2}=(0,0,1)$, $\hat{E}_0=(0,0,1)$, and $\hat{k}_d=(k_{d,1},k_{d,2},0)$. Using Eqs. (19) and (21) one obtains

$$\vec{I}^{T_2}_{\hat{e}\parallel\hat{c}} = (\epsilon_{33}/\epsilon_{11})p'_{44}k_{d,2}(k_{d,1}\vec{I}_2 - k_{d,2}\vec{I}_1) , \tag{50}$$

showing that $\eta=\pi/2$. A look at the scattering kinematics[32,34] readily shows that an interchange of the incident- and scattered-light polarizations implies $E_{0,1}=\pm k_{d,2}$. Consequently, the Brillouin-scattering cross sections (inside the crystal) corresponding to (i) and (ii) are equal. Combining Eqs. (27) and (49) the angular-independent normalized Brillouin-scattering cross section can be written

$$\Sigma^{T_2}_{B,c}(f) \equiv \frac{2\lambda_0 c_{44}\sigma^{T_2}_{B,c}}{\pi^2 n_o^3 n_e^5 (p'_{44})^2 N_R^{T_2}(\vec{q}) k_B T}$$
$$= 1 - \left(\frac{\lambda_0}{2n_o V_p^{T_2}(\pi/2)}\right)^2 f^2 \left[1+\left(\frac{V_p^{T_2}(\pi/2)}{f\lambda_0}\right)^2 (n_o^2-n_e^2)\right]^2 , \tag{51}$$

with the abbreviation $\Sigma^{T_2}_{B,\hat{e}\perp\hat{c}}=\Sigma^{T_2}_{B,\hat{e}\parallel\hat{c}}=\Sigma^{T_2}_{B,c}$. In Fig. 14 is redrawn the normalized cross section obtained by Hamaguchi[33] as a function of the phonon frequency. The low-frequency limit is at $f=(n_e-n_o)V_p^{T_2}(\pi/2)/\lambda_0$, and the high limit at $f=(n_e+n_o)V_p^{T_2}(\pi/2)/\lambda_0$.

D. Scattering on L phonons

When the scattering plane contains the c axis and the incident light is polarized perpendicular to this plane [case (i) of Sec. III B] the normalized frequency-independent Brillouin-scattering cross section is given by

$$\Sigma^{L}_{B,\hat{e}\parallel\hat{s}}(\theta) \equiv \frac{2\lambda_0^4 c_{11}\sigma^{L}_{B,\hat{e}\parallel\hat{s}}}{\pi^2 n_o^8 p_{13}^2 N_L^{L}(\vec{q}) k_B T}$$
$$= \left(\frac{V_p^L(\pi/2)}{V_p^L(\theta)}\right)^2 \left(\frac{p_{12}}{p_{13}}\sin\theta\sin(\theta+\delta)+\cos\theta\cos(\theta+\delta)\right)^2 , \tag{52}$$

as readily can be realized by combining Eqs. (27) and (42), and by noting that the unit-displacement

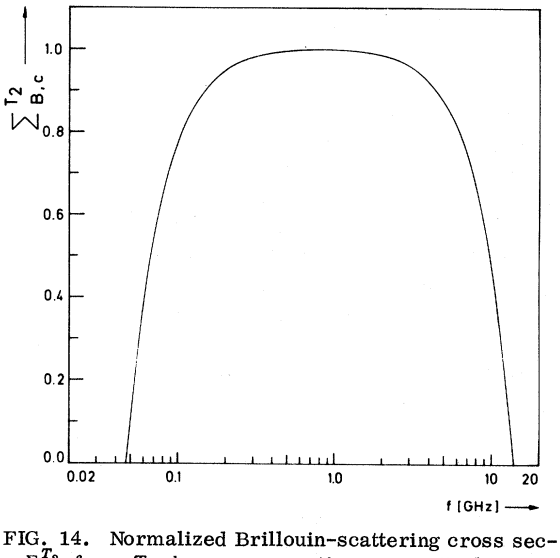

FIG. 14. Normalized Brillouin-scattering cross section $\Sigma^{T_2}_{B,c}$ for a T_2 phonon propagating perpendicular to the optic axis ($\theta=\pi/2$) as a function of the phonon frequency (f) in the case where the basal plane is taken as the scattering plane. The incident photon is polarized either parallel or perpendicular to the c axis (CdS, 300 K, $\lambda_0=6328$ Å.)

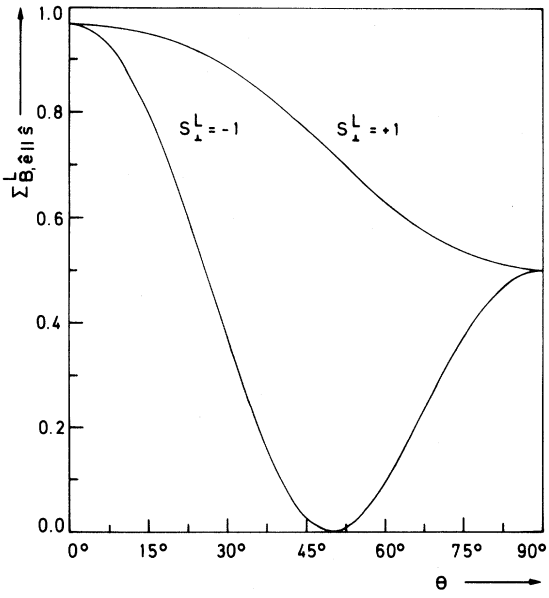

FIG. 15. Frequency-independent normalized Brillouin-scattering cross section $\Sigma^L_{B,\hat{e}\parallel\hat{s}}$ for a L phonon as a function of the phonon off-axis angle (θ). The incident photon is polarized perpendicular to the scattering plane which contains the c axis as shown in Fig. 1. The cross section is plotted for the two possible sign combinations of the involved photoelastic tensor elements, i.e., $S^L_\perp = p_{12}p_{13}/|p_{12}p_{13}| = \pm 1$.

eigenvector for the off-axis quasilongitudinal mode is $\hat{\pi}^L = (\sin(\theta+\delta), 0, \cos(\theta+\delta))$. The normalized cross sections for the two cases $S^L_\perp = p_{12}p_{13}/|p_{12}p_{13}| = \pm 1$ are shown in Fig. 15. Assuming $S^L_\perp = +1$, $\Sigma^L_{B,\hat{e}\parallel\hat{s}}(\theta)$ decreases monotonically between the limits $\Sigma^L_{B,\hat{e}\parallel\hat{s}}(0) = [V^L_p(\pi/2)/V^L_p(0)]^2$ and $\Sigma^L_{B,\hat{e}\parallel\hat{s}}(\pi/2) = (p_{12}/p_{13})^2$. If $S^L_\perp = -1$ the scattering cross section has a zero between these limits at $\theta = \theta_0$, where θ_0 is determined by the implicit equation $A_{13}(\theta_0)\tan\theta_0 = \{[V^L_p(\theta_0)]^2 - A_{11}(\theta_0)\}|p_{13}/p_{12}|$. Neglecting the deviation δ one has $\Sigma^L_{B,\hat{e}\parallel\hat{s}}(\theta) = [V^L_p(\pi/2)/V^L_p(\theta)]^2 [(p_{12}/p_{13})\sin^2\theta + \cos^2\theta]^2$ and $\tan\theta_0 = (|p_{13}/p_{12}|)^{1/2}$. Thus, experimentally obtained Brillouin-scattering intensities from L phonons propagating in a narrow angular range around θ_0 can be used to determine the relative signs of p_{12} and p_{13}. The relative magnitudes of p_{12} and p_{13} can be found by measuring $\Sigma^L_{B,\hat{e}\parallel\hat{s}}(\pi/2)/\Sigma^L_{B,\hat{e}\parallel\hat{s}}(0)$.

Below, we consider case (ii) of Sec. III B, where the incident light is polarized parallel to the scattering plane which contains the c axis. Consistent with the derivation of Eq. (47) we neglect the angular deviation of the L mode from a pure mode and the optical anisotropy of the scattering kinematics. Introducing these justified approximations one obtains, combining Eqs. (27) and (43)–(45), after some trivial calculations the normalized Brillouin-scattering cross section:

$$\Sigma^L_{B,\hat{e}\perp\hat{s}}(f,\theta) \equiv \frac{2\lambda_0^4 c_{11}\sigma^L_{B,\hat{e}\perp\hat{s}}}{\pi^2 n^8 p_{44}^2 N^L_R(\vec{q}) k_B T}$$
$$= \left(\frac{V^L_p(\pi/2)}{V^L_p(\theta)}\right)^2 \left\{\sin^2 2\theta + \left(\frac{p_{31}}{p_{44}}\sin^2\theta + \frac{p_{33}}{p_{44}}\cos^2\theta\right)\right.$$
$$\times \cos 2\theta + \left(\frac{p_{11}+p_{31}}{p_{44}}\sin^2\theta + \frac{p_{13}+p_{33}}{p_{44}}\cos^2\theta\right)$$
$$\left.\times\left[\sin^2\theta - \left(\frac{\lambda_0 f}{2nV^L_p(\theta)}\right)^2\right]\right\}^2. \quad (53)$$

The knowledge of the numerical signs of the symmetric photoelastic tensor elements only implies a calculation of 16 possible scattering cross sections on the basis of Eq. (53).

For $\theta = \pi/4$ the above equation is reduced to

$$\Sigma^L_{B,\hat{e}\perp\hat{s}}(f, \theta=\pi/4) = \left(\frac{V^L_p(\pi/2)}{V^L_p(\pi/4)}\right)^2 \left[1 + \left(\frac{p_{11}+p_{13}+p_{31}+p_{33}}{4p_{44}}\right)\cos 2\Phi^L_B\right]^2, \quad (54)$$

where the Bragg angle corresponding to an isotropic diffraction process is $\Phi^L_B = \arcsin[\lambda_0 f/2nV^L_p(\pi/4)]$. Provided $|4p_{44}/(p_{11}+p_{13}+p_{31}+p_{33})| \leq 1$ the scattering cross section vanishes at a phonon frequency $f = f^L_{\max}(\theta=\pi/4)[1+4p_{44}/(p_{11}+p_{13}+p_{31}+p_{33})]^{1/2}/\sqrt{2}$, where the upper cutoff frequency for the L phonon is $f^L_{\max}(\theta=\pi/4) = 2nV^L_p(\pi/4)/\lambda_0$.

An exact calculation of the Brillouin-scattering cross section valid for an arbitrary magnitude of the optical anisotropy can be obtained for $\theta = 0$ and $\pi/2$. Since $\delta = 0$ in these directions and the pseudomomentum-conservation triangle is isosceles, one finds for $\theta = 0$ on the basis of Eqs. (27) and (43)–(45) the normalized scattering cross section

$$\Sigma^L_{B,\hat{e}\perp\hat{s}}(f, \theta=0) \equiv \frac{2\lambda_0^4 c_{33}\sigma^L_{B,\hat{e}\perp\hat{s}}(f,\theta=0)}{\pi^2 n_e^8 p_{33}^2 N^L_R(\vec{q}) k_B T a}$$
$$= \left\{1 - \left[1 + \frac{p_{13}}{p_{33}}\left(\frac{n_0}{n_e}\right)^4\right]\sin^2(\Phi^L_s/2)\right\}^2$$
$$\times \left\{1 - \left[1 - \left(\frac{n_0}{n_e}\right)^2\right]\sin^2(\Phi^L_s/2)\right\}, \quad (55)$$

where the scattering angle Φ^L_s is given by

$$\sin(\Phi^L_s/2) = \frac{\lambda_0 f}{2n_0 V^L_p(0)} \times \left\{\left(\frac{n_e}{n_0}\right)^2 + \left[1 - \left(\frac{n_e}{n_0}\right)^2\right]\left(\frac{\lambda_0 f}{2n_0 V^L_p(0)}\right)^2\right\}^{-1/2}. \quad (56)$$

Because p_{44} does not appear in the expression for $\Sigma^L_{\hat{e}\perp\hat{s}}(f, \theta=0)$ we have, for convenience, redefined the normalized cross section of Eq. (53). For a small optical anisotropy, i.e., for $|n_e - n_0| \ll n_0$, Eq. (55) is reduced to

$$\Sigma^L_{B,\hat{e}\perp\hat{s}}(f, \theta=0) = \left[1 - \left(1 + \frac{p_{13}}{p_{33}}\right)\left(\frac{\lambda_0 f}{2nV^L_p(0)}\right)^2\right]^2. \quad (57)$$

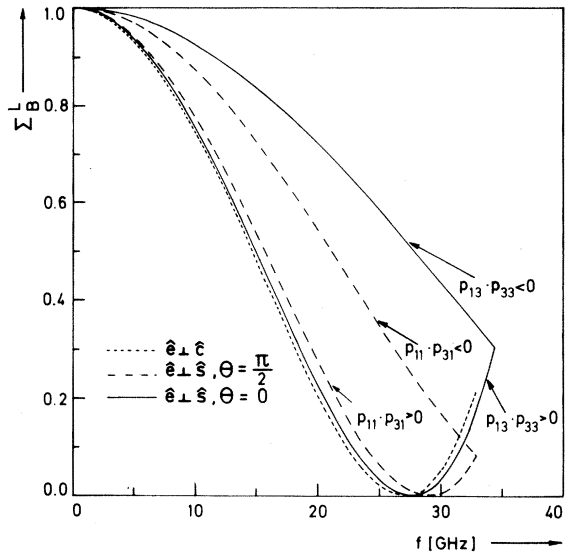

FIG. 16. Normalized Brillouin-scattering cross section Σ_B^L for a L phonon propagating (i) parallel or (ii) perpendicular to the c axis as a function of the phonon frequency (f). The incident photon is in both cases polarized parallel to the scattering plane. In case (ii) the scattering plane either contains the c axis or is perpendicular to it. For the cases where the scattering plane contains the optic axis the cross section has been calculated for the two possible sign combinations of the involved photoelastic tensor elements, i.e., $p_{11}p_{31} \gtrless 0$ and $p_{13}p_{33} \gtrless 0$. (CdS, 300 K, $\lambda_0 = 6328$ Å.)

Based on Eq. (57) we show in Fig. 16 the frequency dependence of $\Sigma^L_{B,\hat{e}\perp\hat{s}}(f, \theta=0)$ in CdS for the two sign combinations $S_{\parallel}^L = p_{13}p_{33}/|p_{13}/p_{33}| = \pm 1$. The values $|p_{13}| = 0.072$ and $|p_{33}| = 0.13$ were taken from Ref. 10. The information that the scattering cross section equals zero for $f = f^L_{\max}(\theta=0)[p_{33}/(p_{13}+p_{33})]^{1/2}$ can be used to measure the relative signs of p_{13} and p_{33}. The relative magnitude of these p's can be found by measuring $\Sigma^L_{B,\hat{e}\perp\hat{s}}(f = f_{\max}(\theta=0), \theta=0)/\Sigma^L_{B,\hat{e}\perp\hat{s}}(f\to 0, \theta=0) = (p_{13}/p_{33})^2$.

For $\theta = \pi/2$ an exact evaluation of the redefined normalized Brillouin-scattering cross section yields

$$\Sigma^L_{B,\hat{e}\perp\hat{s}}(f, \theta=\pi/2) \equiv \frac{2\lambda_0^4 c_{11}\sigma^L_{B,\hat{e}\perp\hat{s}}(f, \theta=0)}{\pi^2 n_o^{10} p_{11}^2 N_R^L(\vec{q}) k_B T a}$$

$$= \left\{1 - \left[1 + \frac{p_{31}}{p_{11}}\left(\frac{n_e}{n_0}\right)^4\right]\sin^2(\Phi_s^L/2)\right\}^2$$

$$\times \left\{1 - \left[1 - \left(\frac{n_e}{n_0}\right)^2\right]\sin^2(\Phi_s^L/2)\right\}, \quad (58)$$

where the scattering angle is obtained from

$$\sin(\Phi_s^L/2) = \frac{\lambda_0 f}{2n_e V_p^L(\pi/2)}$$

$$\times \left\{\left(\frac{n_0}{n_e}\right)^2 + \left[1 - \left(\frac{n_0}{n_e}\right)^2\right]\left(\frac{\lambda_0 f}{2n_e V_p^L(\pi/2)}\right)^2\right\}^{-1/2}. \quad (59)$$

Consistent with the derivation of Eq. (57) the normalized cross section is reduced to

$$\Sigma^L_{B,\hat{e}\perp\hat{s}}(f, \theta=\pi/2)$$

$$= \left[1 - \left(1 + \frac{p_{31}}{p_{11}}\right)\left(\frac{\lambda_0 f}{2n V_p^L(\pi/2)}\right)^2\right]^2 \quad (60)$$

in CdS. Note that the transformation $p_{13}/p_{33} \to p_{31}/p_{11}$ implies $\Sigma^L_{B,\hat{e}\perp\hat{s}}(f, \theta=0) \to \Sigma^L_{B,\hat{e}\perp\hat{s}}(f, \theta=\pi/2)$. The frequency dependence of $\Sigma^L_{B,\hat{e}\perp\hat{s}}(f, \theta=\pi/2)$ is shown in Fig. 16. As in the foregoing case the zero point of the scattering cross section can be used to measure the relative signs of the appropriate p's, and the high- and low-frequency-limit scattering cross section to determine the relative magnitudes of p_{11} and p_{31}.

In the remaining part of this section we consider, for completeness, the case where the scattering plane coincides with the basal plane. The incident light may be polarized (i) parallel to the optic axis or (ii) in the c plane.

(i) $\hat{\kappa} = (1, 0, 0)$, $\hat{\pi}^L = (1, 0, 0)$, $\hat{E}_0 = (0, 0, 1)$, and $\hat{k}_d = (k_{d,1}, k_{d,2}, 0)$. From Eqs. (19) and (21) we obtain

$$\vec{\xi}^L_{\hat{e}\parallel\hat{c}} = p_{31}(\epsilon_{33}/\epsilon_{11})^2 \vec{1}_3 = -\vec{\Xi}^L_{\hat{e}\parallel\hat{c}}, \quad (61)$$

showing that the polarization rotation $\eta = 0$. Inserting the above relation in Eq. (27) one realizes that the direction-independent normalized Brillouin-scattering cross section

$$\Sigma^L_{B,\hat{e}\parallel\hat{c}} \equiv \frac{2\lambda_0^4 c_{11}\sigma^L_{B,\hat{e}\parallel\hat{c}}}{\pi^2 n_e^8 p_{31}^2 N_R^L(\vec{q}) k_B T} = 1 \quad (62)$$

is independent of the phonon frequency.

For the scattering kinematics (ii) $\hat{\kappa} = (1, 0, 0)$, $\hat{\pi}^L = (1, 0, 0)$, $\hat{E}_0 = (E_{0,1}, E_{0,2}, 0)$, and $\hat{k}_d = (k_{d,1}, k_{d,2}, 0)$ one obtains an equation

$$\vec{\Xi}^L_{\hat{e}\perp\hat{c}} = (p_{11}E_{0,1}k_{d,2} - p_{12}E_{0,2}k_{d,1})(k_{d,1}\vec{1}_2 - k_{d,2}\vec{1}_1), \quad (63)$$

which indicates that the scattered light polarization is unrotated ($\eta = 0$) in case (ii). Substituting Eq. (63) into Eq. (27) one finds the following normalized Brillouin-scattering cross section:

$$\Sigma^L_{B,\hat{e}\perp\hat{c}}(f) = \left[1 - \left(1 + \frac{p_{12}}{p_{11}}\right)\left(\frac{\lambda_0 f}{2n_0 V_p^L(\pi/2)}\right)^2\right]^2. \quad (64)$$

A comparison of this equation with Eqs. (57) and (60) shows that the frequency dependence of the scattering cross sections are identical for L phonons propagating parallel to c and L phonons propagating perpendicular to c with a scattering plane which either contains the c axis or is perpendicular to c in CdS if the incident light is polarized in the scattering plane (see Fig. 16). By analogy with the discussion based on Eq. (57) or (60) Eq. (64) should by a suitable experiment enable us to deter-

TABLE I. Normalized Brillouin-scattering cross-section ratios $\Sigma_B^L(f=f_{\max}^L(\theta))/\Sigma_B^L(f=0)$ and $\Sigma_B^L(\theta=\pi/2)/\Sigma_B^L(\theta=0)$, together with zeros for the cross sections for L-phonon scattering in various scattering geometries.

Scattering plane	Polarization of incident light ($\hat{e}$)	θ	Involved photoelastic constants	$\frac{\Sigma_B^L(f=f_{\max}^L(\theta))}{\Sigma_B^L(f=0)}$	$\frac{\Sigma_B^L(\theta=\pi/2)}{\Sigma_B^L(\theta=0)}$	$\Sigma_B^L=0$	
Perpendicular to $\hat{c}$	$\hat{e}\perp\hat{c}$	$\pi/2$	p_{11}, p_{12}	$(p_{11}/p_{12})^2$		$f_{\max}^L(\pi/2)\left(\frac{p_{11}}{p_{11}+p_{12}}\right)^{1/2}$	$p_{11}p_{12}>0$
						no zero	$p_{11}p_{12}<0$
	$\hat{e}\parallel\hat{s}$[a]	$(0\mid\pi/2)$	p_{12}, p_{13}	1	$(p_{12}/p_{13})^2$	no zero	$p_{12}p_{13}>0$
						$\arctan(\lvert p_{13}/p_{12}\rvert)^{1/2}$	$p_{12}p_{13}<0$
Contains $\hat{c}$	$\hat{e}\perp\hat{s}$	0	p_{13}, p_{33}	$(p_{13}/p_{33})^2$		$f_{\max}^L(0)\left(\frac{p_{33}}{p_{13}+p_{33}}\right)^{1/2}$	$p_{13}p_{33}>0$
						no zero	$p_{13}p_{33}<0$
	$\hat{e}\perp\hat{s}$	$\pi/4$	$p_{11}, p_{13}, p_{31}, p_{33}, p_{44}$	$\left(\frac{1-p}{1+p}\right)^2$		no zero	$\lvert p\rvert<1$[b]
						$\frac{1}{2}\sqrt{2}f_{\max}^L(\pi/4)(1+1/p)^{1/2}$	$\lvert p\rvert\geq 1$[b]
	$\hat{e}\perp\hat{s}$	$\pi/2$	p_{11}, p_{31}	$(p_{11}/p_{31})^2$		$f_{\max}^L(\pi/2)\left(\frac{p_{11}}{p_{11}+p_{31}}\right)^{1/2}$	$p_{11}p_{31}>0$
						no zero	$p_{11}p_{13}<0$

[a] $\hat{s}$: unit vector perpendicular to the scattering plane.

[b] $p=\frac{p_{11}+p_{13}+p_{31}+p_{33}}{4p_{44}}$.

mine the relative magnitudes and the signs of the photelastic tensor elements p_{11} and p_{12}.

IV. DETERMINATION OF PHOTOELASTIC TENSOR COMPONENTS FOR $\lvert n_e-n_o\rvert\ll n_o$

An examination of the relative magnitudes and the relative signs of the symmetric photoelastic tensor elements in uniaxial crystals with a small optical anisotropy (CdS, ZnO) can be accomplished by a study of the Brillouin-scattering cross sections for different selected L-phonon diffraction processes. To realize this, we have, on the basis of the results obtained in Sec. III D, set up Table I. It appears that the relative magnitudes of p_{11}, p_{12}, p_{13}, and p_{33} can be evaluated by means of L phonons having off-axis angles $\theta=0$ and $\pi/2$. For the frequency-dependent Brillouin-scattering cross sections one measures the relative cross sections for the collinear diffraction processes having $\Phi_s=0$ and π. For the frequency-independent cross section one determines the ratio of the L-phonon cross sections in the directions $\theta=0$ and $\pi/2$. Before one can calculate the relative magnitude of p_{44} the relative signs of p_{11}, p_{13}, p_{31}, and p_{33} must be determined. This is done by investigating whether the appropriate scattering cross sections vanish for the phonon frequencies or the phonon off-axis angle given in the last column of Table I. From a knowledge of the relative signs and magnitudes of p_{11}, p_{13}, p_{31}, and p_{33} the relative magnitude and sign of p_{44} can be evaluated from a measurement of the ratio $\Sigma_{B,\hat{e}\perp\hat{s}}^L(\Phi_s=\pi,\ \theta=\pi/4)/\Sigma_{B,\hat{e}\perp\hat{s}}^L(\Phi_s=0,\ \theta=\pi/4)=[(1-p)/(1+p)]^2$, where $p=(p_{11}+p_{13}+p_{31}+p_{33})/4p_{44}$. Note that the deviation of the L mode from a pure mode has been neglected in the setting up of the table.

According to the treatment in Secs. III A–III D, it is obvious that the photoelastic tensor elements can be determined in several ways. The method sketched above is, however, especially simple since it is based on the use of only one phonon type which propagates in the special directions given by $\theta=0$, $\pi/4$, and $\pi/2$.

V. LINKS BETWEEN THEORY AND EXPERIMENT

The Brillouin-scattering theory outlined in Secs. II and III enables one to calculate the intensity inside the crystal of light scattered from a single thermal or nonthermal acoustic mode through a Stokes or an anti-Stokes process.

From an experimental point of view it is important to couple the scattered radiation from the inside to a detector outside the scattering medium. This problem is, in principle, trivial but involves for many commonly used geometries a number of lengthy calculations. Thus, when considering the reflection and refraction effects at the surfaces of the sample, we have to take into account a possible

polarization rotation of the scattered light, and multiple internal reflections of both scattered and unscattered light beams,[19] if we are dealing with the case of weak scattering.[17] Besides these Fresnels corrections solid-angle expansion[12] and source demagnification[12] must be considered. Consideration of these effects is complicated in the general case by the noncollinearity of wave vectors and Poynting vectors and by astigmatism introduced by the planar exit surface. To determine the solid-angle expansion one must relate the solid angle in free space subtended by the detector to a solid-angle element of the wave vectors inside the medium. In turn, this element must be related to the element $d\Omega$ of solid angle of Poynting vector directions given in Sec. II. An important implication of the above considerations is that the Stokes and anti-Stokes intensities in general are different outside the crystal.

A Brillouin-scattering investigation of on-axis[17,19] or off-axis[20] acoustoelectric domains involves a study of an amplified portion of the thermal-phonon distribution. As pointed out by Spears[17] the angular dependence of the scattered intensity does not reflect the spectral distribution of the acoustic energy in this case, or in the case where the scattering takes place from a thermal-phonon distribution. According to the Debye theory, the number of acoustic modes per unit frequency bandwidth is proportional to the square of the acoustic frequency f. Thus, to obtain the spectral distribution of the acoustic energy an f^2 correction must be made, provided the volume of space probed by the light beam falls well within the cone of the amplified phonon beam. If this is not the case, the frequency resolution and the angular resolution, especially for optically anisotropic crystals, can give rise to more complicated conversion factors.

ACKNOWLEDGMENTS

The author is indebted to C. Søndergaard for his continuous assistance in a number of numerical calculations and to Professor K. Maack Bisgård for his interest and support of this work.

APPENDIX

An extensive analysis of the lossless propagation characteristics of elastic waves in hexagonal crystals has been given by Musgrave.[46] In the following we summarize the main properties of elastic waves propagating in arbitrary crystallographic directions.

The phase velocity and polarization of the acoustic modes can be determined by solving the eigenvalue problem

$$\sum_{j,k,l=1}^{3} c_{ijkl}\kappa_j\kappa_l\pi_k = V_p^2\pi_i\,, \tag{A1}$$

where c_{ijkl} is the components of the elastic-stiffness tensor. For an acoustic wave vector forming an angle θ with the c axis we obtain the three orthogonal unit-displacement eigenvectors

$$\hat{\pi}^{T_1} = (0, 1, 0), \quad \text{pure transverse mode} \tag{A2}$$

$$\hat{\pi}^{T_2} = (\cos(\theta+\delta), 0, -\sin(\theta+\delta)), \quad \text{quasitransverse mode} \tag{A3}$$

$$\hat{\pi}^{L} = (\sin(\theta+\delta), 0, \cos(\theta+\delta)), \quad \text{quasilongitudinal mode.} \tag{A4}$$

The deviation (δ) of the T_2 and L modes from pure modes is given by

$$\delta = -\theta + \arctan\left(\frac{A_{13}}{(V_p^L)^2 - A_{11}}\right)\,, \tag{A5}$$

and the phase velocities of the three modes are

$$V_p^{T_1} = (A_{22})^{1/2} \tag{A6}$$

and

$$V_p^{T_2,L} = \left\{ \frac{A_{11}+A_{33}}{2} \mp \left[\left(\frac{A_{11}-A_{33}}{2}\right)^2 + A_{13}^2\right]^{1/2} \right\}^{1/2}, \tag{A7}$$

where

$$A_{11} = (1/\rho)(c_{11}\sin^2\theta + c_{44}\cos^2\theta),$$

$$A_{22} = (1/\rho)[\tfrac{1}{2}(c_{11}-c_{12})\sin^2\theta + c_{44}\cos^2\theta]$$

$$A_{33} = (1/\rho)(c_{44}\sin^2\theta + c_{33}\cos^2\theta),$$

$$A_{13} = (1/\rho)(c_{13}+c_{44})\sin\theta\cos\theta.$$

In Sec. III, we have used the following data (contracted notation) for CdS at 300 K[47]: $c_{11} = 8.581 \times 10^{10}\ \mathrm{N/m^2}$, $c_{12} = 5.334 \times 10^{10}\ \mathrm{N/m^2}$, $c_{13} = 4.615 \times 10^{10}\ \mathrm{N/m^2}$, $c_{33} = 9.370 \times 10^{10}\ \mathrm{N/m^2}$, and $c_{44} = 1.487 \times 10^{10}\ \mathrm{N/m^2}$.

[1] L. Brillouin, Ann. Phys. (Paris) 17, 88 (1922).
[2] P. Debye and F. W. Sears, Proc. Natl. Acad. Sci. USA 18, 409 (1932).
[3] R. Lucas and P. Biquard, J. Phys. Rad. 3, 464 (1932).
[4] H. Bommel and K. Dransfeld, Phys. Rev. Lett. 1, 234 (1958).
[5] G. Benedek, J. B. Lastovka, K. Fritsch, and T. Greytak, J. Opt. Soc. Am. 54, 1284 (1964).
[6] R. Y. Chiao and B. Stoicheff, J. Opt. Soc. Am. 54, 1286 (1964).
[7] D. I. Mash, V. S. Starunov, and I. Fabelinskii, Zh. Eksp. Teor. Fiz. 47, 783 (1964) [Sov. Phys. - JETP 20, 523 (1965)].
[8] G. Benedek and T. Greytak, Proc. IEEE 53, 1623 (1965).
[9] D. H. McMahon, IEEE Trans. SU-14, 103 (1967).

[10]W. T. Maloney and H. R. Carleton, IEEE Trans. SU-14, 135 (1967).
[11]R. W. Dixon, J. Appl. Phys. 38, 5149 (1967).
[12]D. F. Nelson, P. D. Lazay, and M. Lax, Phys. Rev. B 6, 3109 (1972).
[13]J. Zucker and S. Zemon, Appl. Phys. Lett. 9, 398 (1966).
[14]B. W. Hakki and R. W. Dixon, Appl. Phys. Lett. 14, 185 (1969).
[15]W. Wettling and M. Bruun, Phys. Status Solidi 34, 221 (1969).
[16]A. Ishida and Y. Inuishi, J. Phys. Soc. Jap. 26, 957 (1969).
[17]D. L. Spears, Phys. Rev. B 2, 1931 (1970).
[18]E. D. Palik and R. Bray, Phys. Rev. B 3, 3302 (1971).
[19]M. Yamada, C. Hamaguchi, K. Matsumoto, and J. Nakai, Phys. Rev. B 7, 2682 (1973).
[20]O. Keller, Phys. Rev. B 10, 1585 (1974).
[21]S. Zemon and J. Zucher, IBM J. Res. Dev. 13, 494 (1969).
[22]M. Bruun, W. Wettling, and N. I. Meyer, Phys. Lett. A 31, 31 (1970).
[23]O. Keller, Phys. Status Solidi A 10, 581 (1972).
[24]M. Sanya, M. Yamada, C. Hamaguchi, and J. Nakai, Jap. J. Appl. Phys. 13, 611 (1974).
[25]O. Keller, Phys. Status Solidi A 16, 87 (1973).
[26]O. Keller, Solid State Commun. 13, 1541 (1973).
[27]F. Siebert, O. Keller, and W. Wettling, Phys. Status Solidi A 4, 67 (1971).
[28]O. Keller, Phys. Lett. A 39, 235 (1972).
[29]A. R. Moore, Appl. Phys. Lett. 13, 126 (1968).
[30]Y. Mita, J. Appl. Phys. 42, 2886 (1971).
[31]O. Keller, Phys. Lett A 43, 65 (1973).
[32]O. Keller and C. Søndergaard, Jpn. J. Appl. Phys. 13, 1765 (1974).
[33]C. Hamaguchi, J. Phys. Soc. Jap. 35, 832 (1973).
[34]R. W. Dixon, IEEE J. Quantum Electron. 3, 85 (1967).
[35]H. Küppers, Phys. Status Solidi 37, K 59 (1970).
[36]L. L. Hope, Phys. Rev. 166, 883 (1968).
[37]G. B. Benedek and K. Fritsch, Phys. Rev. 149, 647 (1966).
[38]C. F. Quate, C. D. W. Wilkinson, and D. K. Winslow, Proc. IEEE 53, 1604 (1965).
[39]F. Pöckels, Ann. Phys. 37, 144 (1889); 37, 269 (1889); 37, 372 (1889); 39, 440 (1890).
[40]D. F. Nelson and M. Lax, Phys. Rev. Lett. 24, 379 (1970).
[41]J. Chapelle and L. Taurel, C. R. Acad. Sci. (Paris) 240, 743 (1955).
[42]O. Keller (unpublished).
[43]W. Wettling (private communications).
[44]O. Keller (unpublished).
[45]J. M. Ziman, *Electrons and Phonons* (Clarendon, Oxford, England, 1960).
[46]M. J. P. Musgrave, Rep. Prog. Phys. 22, 74 (1965).
[47]H. J. McSkimmin, T. B. Bateman, and A. R. Hutson, J. Acoust. Soc. Am. 33, 856 (1961).